GEOLOGICA CARPATHICA, AUGUST 2008, 59, 4, 277–293

Amphibole gabbroic rocks from the Mt Medvednica ophiolite mélange (NW Croatia): geochemistry and tectonic setting

DAMIR SLOVENEC[1] and BOŠKO LUGOVIĆ[2]

[1]Croatian Geological Survey, Sachsova 2, HR-10000 Zagreb, Croatia; damir.slovenec@hgi-cgs.hr
[2]Institute of Mineralogy, Petrology and Mineral Deposits, Faculty of Mining, Geology and Petroleum Engineering, University of Zagreb, Pierottijeva 6, HR-10000 Zagreb, Croatia; blugovic@rgn.hr

(Manuscript received December 27, 2007; accepted in revised form March 31, 2008)

Abstract: Amphibole gabbroic rocks with heteradcumulate and isotropic fabric constitute centimeter to hectometer large fragments in the Early Callovian to the Late Valanginian ophiolite mélange of the Mt Medvednica located at the SW tips of the Zagorje-Mid-Transdanubian Shear Zone. Normalized multielement concentration patterns have strong Ta-Nb anomaly [$(Nb/La)_{MORBN} = 0.28–0.72$] for all rocks, while normalized REE concentration of isotropic gabbros show patterns transitional between mid-ocean ridge and island arc magmatic rocks [$(La/Lu)_{MORBN} = 0.92–1.12$]. Low Ti, Cr and Na content of clinopyroxene from the isotropic gabbros (< 0.98 wt. % TiO_2, < 0.94 wt. % Cr_2O_3, < 0.39 wt. % Na_2O) combined with high Ca-plagioclase (up to An_{93}) and crystallization of plagioclase after augite-diopside with tschermakite-magnesiohornblende as intercumulus oikocrystal bring in the evidence of formation in a suprasubduction setting. The rocks were severely albitized and uralitized in greenschist facies on the sea floor and altered in prehnite-pumpellyite facies during emplacement. Due to the alterations the LILE may have been selectively enriched while HFSE and REE retained magmatic ratios. Overall geochemical data and age determination of gabbropegmatite (161.1 Ma) are liable to geotectonic constraints and advocate a proto-arc–immature intra-oceanic island arc source of the Mt Medvednica gabbroic fragments. It was suggested that the Mt Medvednica gabbroic rocks represent remnants of an extinct intra-oceanic arc system formed in the Repno domain of the Neotethyan oceanic realm. A petrogenetic and geotectonic connection between the Repno and Maliak-Dinaric oceanic domains cannot be positively postulated on the basis of the presented data.

Key words: Croatia, Zagorje-Mid-Transdanubian Shear Zone, Mt Medvednica, island arc, amphibole gabbros, ophiolite mélange.

Introduction

An ophiolite mélange is a tectono-sedimentary unit initially accreted in a deep ocean trench (accretionary wedge) over a subducting plate in front of the leading edge of the overriding plate. The mélange is an archive of very heterogeneous rock fragments, derived from both sides of the accretionary wedge, representing remnants of different tectonostratigraphic units formed during the long lasting evolution of an oceanic system. Systematic petrological and geochemical analyses of these rocks fragments give an opportunity to study the history of an oceanic system from the steady state oceanic crust formation to the final closure. This method is particularly efficient when regional field relations fail to resolve the geotectonic affiliation of poorly exposed ophiolitic rocks as confirmed in the Panonnian Basin and Sava Zone.

Mt Medvednica is located on the southernmost segment of the Zagorje-Mid-Transdanubian Shear Zone (ZMTDZ) and exposes one of the largest ophiolitic mélanges in the entire Pannonian Basin and NW Sava Zone. The Mt Medvednica ophiolite mélange is peculiarly positioned between the Maliak ophiolites to the NW and Dinaric/Vardar ophiolites to the SE (Fig. 1A). The mélange consists of remnants of Mesozoic oceanic crust along with fragments of sedimentary rocks derived from different geotectonic provenances (Slovenec 1998, 2003; Slovenec & Pamić 2002, and references therein).

The fragments of cumulus and isotropic gabbroic rocks with magmatic amphibole are relatively widespread in the Mt Medvednica ophiolite mélange (Crnković 1963; Slovenec & Pamić 2002). Amphibole mafic intrusives have particular importance in the study of ophiolites because they are diagnostic for suprasubduction origin of an ancient oceanic crust. However, detailed study of the petrological and geochemical characteristics of the Mt Medvednica amphibole gabbroic rocks have not been performed yet.

The aim of this paper is to give overall petrological and geochemical characteristics of the Mt Medvednica amphibole gabbroic rocks to determine their petrogenesis and to suggest the probable geotectonic setting of their formation. For the first time we present the evidence for the existence of a proto-arc–island arc system in the ZMTDZ. Finally, we correlate the Mt Medvednica gabbroic rocks with equivalent rocks from the Szarvaskő ophiolites at Bükk Mts in NE Hungary and the Meliata ophiolites at Jaklovce intending to figure out their potential geotectonic link.

Geological setting

Mt Medvednica is located on the ZMTDZ segment of the Sava Zone (Fig. 1A,B). This part of the Sava Zone represents the area of the triple junction of the Southern-Eastern Alps, Tisia block of the Pannonian Basin and the Internal Di-

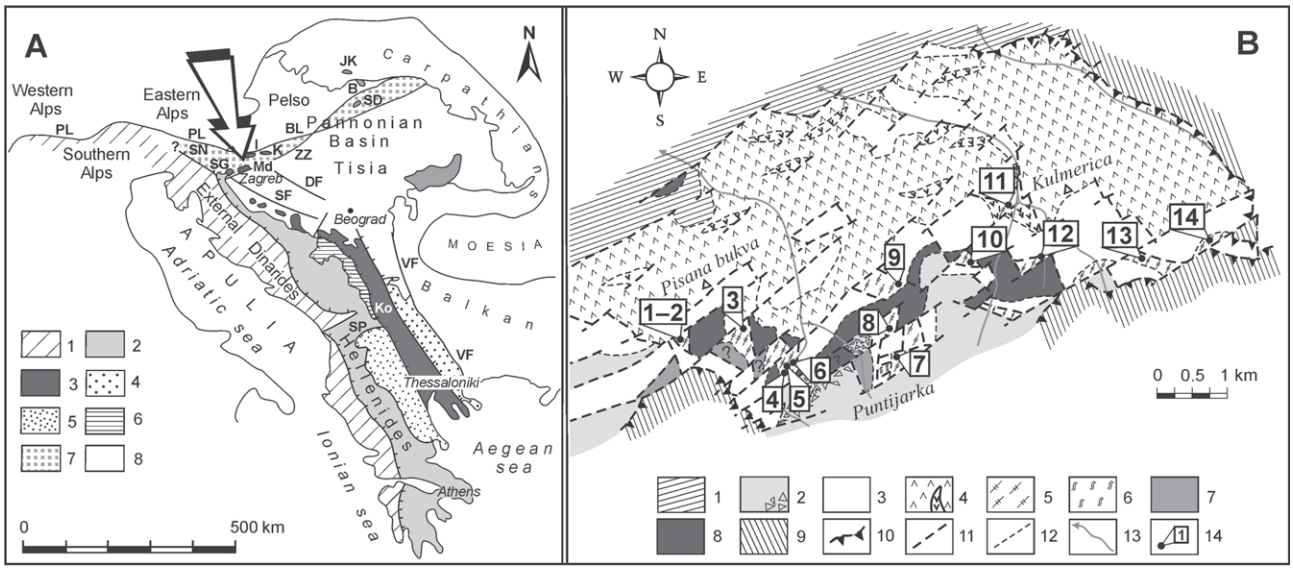

Fig. 1. A — Geotectonic sketch map of the Alps, Dinarides and Hellenides showing the position of the Periadriatic-Sava-Vardar suture zone (after Pamić 2000). Legend: 1 — External units (External Dinarides and Alps); 2 — Internal units [Passive continental margin, Central Dinaride Ophiolite Belt (CDOB), Mirdita Zone]; 3 — Periadriatic-Sava-Vardar Zone; 4 — Serbo-Macedonian Massif; 5 — Pelagonides; 6 — Golija Zone; 7 — Zagorje-Mid-Transdanubian Zone; 8 — Panonian Basin. Faults: BL — Balaton; DF — Drava; PL — Periadriatic; SF — Sava; SP — Skadar-Peć; SN — Sava Nape; VF — Vardar; ZZ — Zagreb-Zemplin. Mountains: I — Ivanščica; K — Kalnik; Ko — Kopaonik; Md — Medvednica; SG — Samoborska Gora; SD — Szarvaskő-Darnó; B — Bódva valley; JK — Jaklovce. **B** — Simplified geological map of Mt Medvednica (modified after Halamić 1998). Legend: 1 — Neogene and Pleistocene sedimentary rocks; 2 — Late Cretaceous-Paleocene flysch including Senonian carbonate breccias; 3 — ophiolite mélange with blocks of: 4 — basalt intersected by dolerite dikes, 5 — gabbros, 6 — cumulate peridotites, 7 — Jurassic radiolarites and shales with olistoliths composed of basalts; 8 — Alb-Cenomanian limestones and clastic rocks (shale, siltite and sandstone); 9 — Lower Cretaceous metamorphic complex; 10 — reverse or thrust faults; 11 — normal faults; 12 — geological contact line; 13 — main creeks; 14 — sample location (1 = mc-16; 2 = mc-pg; 3 = vs-801; 4 = vs-335; 5 = m-16/2; 6 = vs-331; 7 = vs-367; 8 = vs-386; 9 = vk-298; 10 = mc-2/4; 11 = rn-13; 12 = vs-494; 13 = vh-617; 14 = vs-578).

narides and consists of mixed and superimposed Dinaric and Alpine tectonostratigraphic and tectonometamorphic slices of still debatable origin (Pamić & Tomljenović 1998; Herak 1999; Haas et al. 2000; Haas & Kovács 2001; Pamić 2002, 2003). The low-grade metamorphic unit of Early Aptian age (Belak et al. 1995) are derived from the protoliths of Silurian to Ladinian volcano-sedimentary successions and from Middle Jurassic–Lower Cretaceous island arc volcanics (Lugović et al. 2006, and references therein). In the recent structural assemblage this low-grade metamorphic complex thrusts over the ophiolite mélange. The accretion age of the ophiolite mélange was constrained by palynomorph assemblages as Middle Jurassic to Hauterivian (Babić et al. 2002). Both units are covered by Cretaceous-Paleocene alluvial fan to flysch sequences. These successions form the base of the transgressive Neogene sedimentary sequence composed of Miocene limestones, clastics and marls. The pre-Neogene Mt Medvednica basement is believed to have experienced long distance transport from the NW and was rotated during the Oligocene by ca. 100° CW to the alignment perpendicular to the Dinaric structural trend in the SE (Tomljenović 2002; Tomljenović et al. 2008) (Fig. 1A).

Within the pelitic-siltous matrix the Mt Medvednica ophiolite mélange archives variously sized rock fragments of very different tectonic settings. Gabbroic cumulus and isotropic rocks form decimeter to hectometer large fragments within the Mt Medvednica ophiolite mélange (Fig. 1B). Large gabbroic blocks are locally intersected by gabbropegmatite veins, or may contain their segregations and ooze. Most rock fragments are not suitable for paleontological or geochemical dating (Halamić 1998).

The oldest blocks in the mélange are olistoliths of Illyrian-Fassanian pelagic limestones associated with MORB-pillow lavas (Halamić et al. 1998) and, fragments of Middle to Upper Triassic limestones interlayered with radiolarian cherts (Halamić & Goričan 1995). The uppermost Bajocian to Lower Callovian radiolarian cherts are also found in the Mt Medvednica ophiolite mélange together with MORB-pillow lavas as slices which were assumed to record an oceanic ridge relationship (Halamić et al. 1999). The age span of the K-Ar data (196–179 Ma) performed on the MORB-type gabbro and dolerite (Pamić 1997) revealed that the oceanic crust formed within the same paleogeographical domain also between the Pliensbachian and Bajocian. The Middle Jurassic to Hauterivian ophiolitic mélange as a tectonic formation was involved in Aptian to post-Paleocene emplacement onto the eastern continental margin of the Adria plate (Pamić & Tomljenović 1998; Pamić 2002). However, the ophiolite emplacement which resulted in obduction of mantle peridotite took place before the Senonian as is clearly seen from the mantle peridotite clasts documented in the Campanian basal conglomerates (Halamić 1998) and by subaerial weathering to the Ni-lateritic crust (Palinkaš et al. 2006).

Analytical techniques

Eight samples were selected for the analysis of mineral chemistry. The minerals were analysed with Camebax SX51 microprobe equipped with five wavelength spectrometers at the Mineralogisches Institut, Universität Heidelberg. The elements were measured by WDS with an accelerating voltage of 15 kV, beam current of 20 nA, ~1 μm beam size and 10 s counting time for all elements. For feldspars an analysis beam size of 10 μm was used. Natural oxides (corundum, spinels, hematite and rutile) and silicates (albite, orthoclase, anorthite and wollastonite) were used as standards and for calibration. Raw data for all analyses were corrected for matrix effects with the PAP algorithm (Pouchou & Pichoir 1984, 1985) implemented by CAMECA. Calculations of the structural chemical formulas were done using a software package authorized by Hans-Peter Mayer (Mineralogisches Institut University of Heidelberg).

The total of twelve representative samples were crushed in a steel jaw. After splitting, rock chips free of visible vein and crack fillings were ground in an agate ring-disc mill, and powders were then dried at 110 °C. Three samples were analysed for the major elements and trace elements Rb, Ba, Sr, Zr, Y and Cr at XRAL Laboratories at Toronto (Canada) by wavelength dispersive X-ray fluorescence (WDS XRF) on lithium borate fusion pellets using international reference samples for calibration. Trace elements (Th, Nb, Ta, Hf, Sc, V, Co, Ni, Zn and REE) of those samples were determined by inductively coupled plasma mass spectrometry (ICP-MS) at ACME Laboratories in Vancouver, Canada. Another set of nine samples were analysed by ICP for major elements, and ICP-MS for all trace elements at Actlab Laboratories in Ancaster, Canada.

Amphibole separate from gabbropegmatite (sample mc-pg) was prepared by crushing and sieving the grain fraction 200–400 μm followed by magnetic separation and final handpicking under stereomicroscope. The amphibole separate was wrapped in aluminium foil and stacked in an irradiation capsule with similar-aged samples and neutron flux monitors (Fish Canyon Tuff sanidine). Samples were irradiated at the McMaster Nuclear Reactor in Hamilton, Ontario and analysed at the Noble Gas Laboratory Pacific Centre for Isotopic and Geochemical Research, University of British Columbia, Vancouver, Canada. The samples were step-heated at incrementally higher powers in the defocused beam of a 10 W CO_2 laser until fused. The gas evolved from each step was analysed by a VG5400 mass spectrometer equipped with an ion-counting electron multiplier.

Petrography and mineral chemistry

The gabbroic rocks of Mt Medvednica are medium- to coarse-grained (1–4 mm) and may contain 1–5 cm large grains in the gabbropegmatite. The rocks preserve igneous fabric in spite of being successively altered. Amphibole gabbro dominates over amphibole- olivine-gabbro and minor gabbropegmatite. The rocks are isotropic and only a few samples show heteradcumulate poikilitic texture with large oikocrystals of brown-reddish amphibole enclosing fresh cumulus clinopyroxene (Fig. 2A) or albitized plagioclase (Fig. 2B). Occasionally, olivine pseudomorphosed by serpentine and magnetite is also embedded by amphibole. The crystallization sequence includes olivine, augite, plagioclase, reddish-brown amphibole and Fe-Ti oxide (magnetite-ulvöspinel). Plagioclase forms oikocrystals in cumulate olivine-gabbros. Poikilitic embedding of plagioclase and amphibole suggests their cotectic crystallization. Detailed petrography of these rocks may be found in Slovenec (1998).

The cumulus clinopyroxene embedded in the amphibole oikocrysts (see Fig. 2) ranges in composition from augite to diopside ($Wo_{42-49}En_{42-50}Fs_{6-14}$; Fig. 3). A reaction relation of augite with enclosing amphibole was not observed. The clinopyroxene from the gabbroic cumulates shows Mg# of 75.8–88.9 suggesting that the most evolved composition fractionated from a melt having Mg# of around 39 [calculated on K_d (= cpx/bulk rock FeO_{tot}/MgO molar ratio) of 0.20 after Grove et al. (1982); Baker & Eggler (1987)]. Abundances of Ti, Al, Cr and Na are low (< 0.64 wt. % TiO_2;

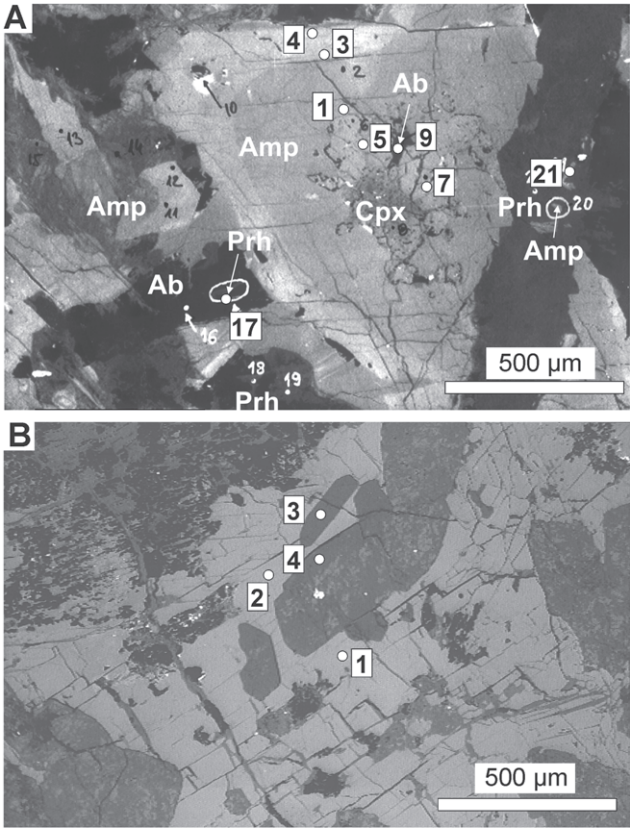

Fig. 2. Back-scattered electron image of **(A)** cumulus gabbro, sample mc-16, showing large oikocrystal of zoned tschermakite-magnesiohornblende enclosing cumulus clinopyroxene surrounded by various alterations minerals. The numbers correspond to the microprobe spot analyses as indicated in the tables of mineral chemistry (for example: 1 — tschermakite, 2 and 3 — magnesiohornblende, 4 — actinolite). Legend: Ab = albite; Amp = amphibole; Cpx = clinopyroxene; Prh = prehnite. **(B)** cumulus gabbro, sample vh-617, showing albitized cumulus plagioclase (spots 3 and 4) enclosed in large intercumulus oikocrystal of magnesiohornblende (spots 1 and 2).

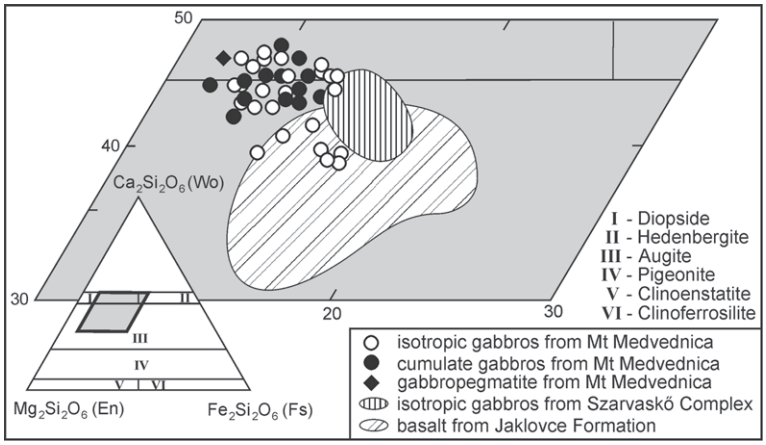

Fig. 3. Plot of clinopyroxene compositions in the En–Wo–Fs ($Mg_2Si_2O_6$–$Ca_2Si_2O_6$–$Fe_2Si_2O_6$) diagram with the nomenclature fields of Morimoto (1988) for gabbroic rocks from the Mt Medvednica ophiolite mélange. Fields for clinopyroxene compositions from isotropic gabbros of Szarvaskő Ophiolite Complex (Balla & Dobretsov 1984) and basalts from the Jaklovce Formation (Hovorka & Spišak 1988; Ivan 2002) plotted for correlation constraints.

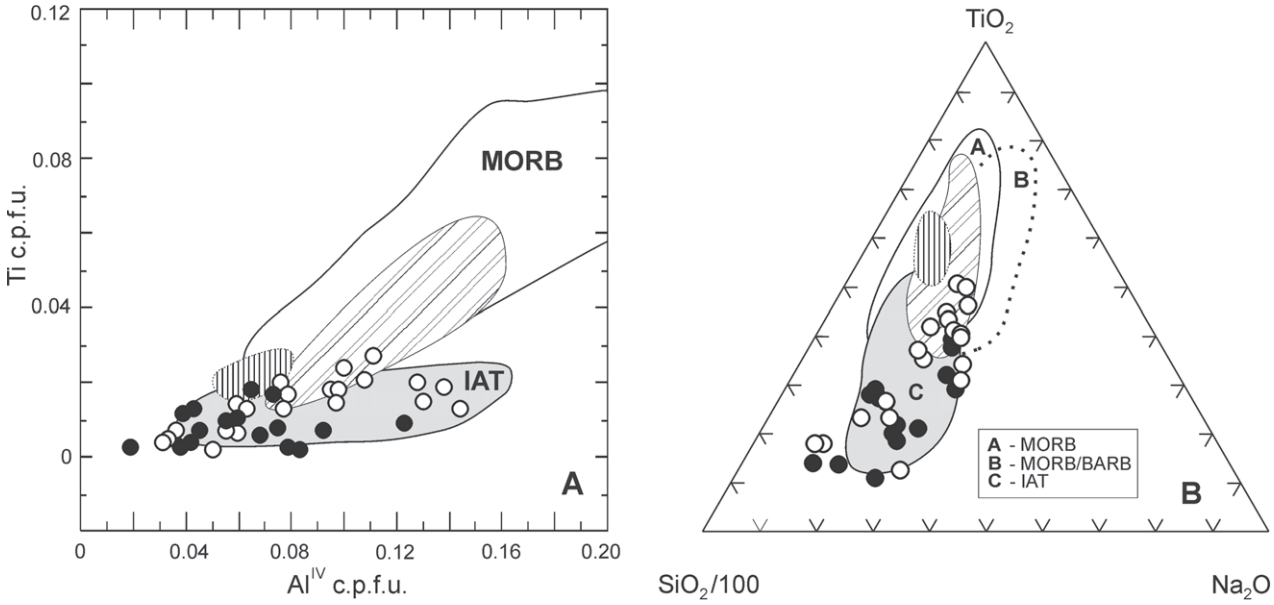

Fig. 4. Discriminant diagram **(A)** Ti–Al^{IV} and **(B)** SiO_2/100–Na_2O–TiO_2 (simplified after Beccaluva et al. 1989) for clinopyroxene from the Mt Medvednica gabbros. For convenience cumulus pyroxenes are also plotted although they were not considered in geotectonic constraints. IAT = island-arc tholeiites, MORB = mid-ocean ridge basalts, BARB = back-arc ridge basalts. Symbols and fields as in the Fig. 3.

<2.41 wt. % Al_2O_3; <0.51 wt. % Cr_2O_3; <0.38 wt. % Na_2O; Table 1). The clinopyroxene from isotropic gabbros has a composition of $Wo_{39-48}En_{40-49}Fs_{8-19}$, similar to the composition of cumulus clinopyroxene (Fig. 3; Table 1). However, they are slightly enriched in all non-quadrilateral components (Fig. 4A,B) except Na_2O which is identical (<0.97 wt. % TiO_2; <4.16 wt. % Al_2O_3; wt. % 1.01 Cr_2O_3; Table 1). The Al^{VI}/Al^{IV} ratio of cumulus clinopyroxene does not exceed 0.73 which is typical of clinopyroxene from low to medium pressure igneous rocks (Aoki & Kushiro 1968; Wass 1979). The Al^{VI}/Al^{IV} ratio of clinopyroxene from isotropic gabbros is low (<0.56), consistent with their position higher in the ophiolite pile.

All analysed amphiboles show Mg# [=Mg/(Mg+Fe^{2+})] of 0.591–0.868 and belong to the Ca-amphibole group (Table 2; Fig. 5). Magnesiohornblende oikocrystal embaying albitized plagioclase in a cumulus gabbro (Fig. 2B) has homogeneous composition across the grain (Table 2) whilst amphibole oikocrystal in the sample mc-16 (Fig. 2A) shows three generations rimward: (1) reddish-brown igneous tschermakite enclosing cumulus augite, (2) brown magnesiohornblende as the late stage crystallization to deuteric product, and (3) pale green actinolite as low temperature alteration of brown magnesiohornblende (Table 2, Fig. 2A and Fig. 5). The zoning pattern of a tschermakite from the gabbropegmatite showing decreasing Ti, Al and Na towards the grain periphery (Fig. 6) is typical of fractional crystallization. Amphiboles (1) and (2) in the sample mc-16 resemble the fractionation pattern of tschermakite megacryst from the gabbropegmatite confirming their igneous origin. Tschermakite in the cumulus rocks is characterized by high Ti and Al contents compared to the late magmatic magnesiohornblende (2.84–3.77 wt. % TiO_2 vs. 1.22–2.66 wt. % TiO_2 and 9.43–11.14 wt. % Al_2O_3 vs. 5.52–8.80 wt. % Al_2O_3), and par-

Table 1: Selected microprobe analyses and formulae of clinopyroxene from the gabbroic rocks in the Mt Medvednica ophiolite mélange.

Sample	mc-16	mc-16	vs-386	vs-386	vs-386	m-16/2	m-16/2	m-16/2	vs-331	vs-331	vs-494	vs-494	vs-578	vs-578	vs-578	vs-578
Anal. No.	7	5	2	14	18	4	13	17	11	13	4	11	2	4	13	14
Rock type	CG		CG			CG			IG				IG			
SiO_2	52.44	51.99	52.34	53.38	52.59	53.71	52.74	53.50	50.86	50.73	53.17	53.25	50.99	50.95	50.70	52.61
TiO_2	0.47	0.63	0.09	0.21	0.10	0.12	0.30	0.13	0.53	0.65	0.16	0.24	0.67	0.87	0.67	0.48
Al_2O_3	1.68	2.30	2.28	1.96	2.02	0.45	1.51	1.28	4.16	2.52	1.03	1.29	2.31	2.68	3.92	1.80
Cr_2O_3	0.06	0.20	0.12	0.42	1.09	0.00	0.02	0.00	0.93	0.09	0.05	0.14	0.03	0.01	0.62	0.08
Fe_2O_3	0.21	0.45	2.47	1.61	1.72	0.59	1.37	1.06	1.79	2.46	0.91	0.27	2.67	2.18	2.82	1.30
FeO	8.03	7.67	2.76	2.45	2.37	5.36	7.37	6.11	3.96	6.88	4.20	5.23	7.79	9.19	3.95	6.41
MnO	0.21	0.20	0.16	0.15	0.14	0.20	0.21	0.15	0.14	0.31	0.16	0.19	0.40	0.32	0.15	0.17
MgO	14.63	14.64	17.91	17.64	17.49	15.08	15.14	15.87	16.31	13.96	15.84	16.62	15.10	14.67	16.16	17.31
CaO	21.29	21.26	21.24	22.60	22.17	24.64	21.98	22.66	20.57	21.46	24.04	22.04	19.46	18.95	20.80	19.35
Na_2O	0.33	0.33	0.13	0.22	0.19	0.07	0.13	0.11	0.38	0.36	0.07	0.13	0.33	0.38	0.36	0.24
Total	99.35	99.66	99.51	100.64	99.88	100.22	100.77	100.87	99.63	99.43	99.63	99.40	99.75	100.20	100.15	99.75
Si	1.958	1.935	1.917	1.932	1.921	1.981	1.944	1.958	1.870	1.903	1.962	1.964	1.904	1.900	1.862	1.937
Ti	0.013	0.018	0.002	0.006	0.003	0.003	0.008	0.004	0.015	0.018	0.004	0.007	0.019	0.024	0.019	0.013
Al^{IV}	0.042	0.065	0.083	0.068	0.079	0.019	0.056	0.042	0.130	0.097	0.038	0.036	0.096	0.100	0.138	0.063
Al^{VI}	0.032	0.035	0.016	0.016	0.008	0.001	0.010	0.013	0.051	0.014	0.007	0.020	0.006	0.018	0.031	0.015
Cr	0.002	0.006	0.003	0.012	0.031	0.000	0.001	0.000	0.027	0.003	0.001	0.004	0.001	0.000	0.018	0.002
Fe^{3+}	0.006	0.013	0.068	0.044	0.047	0.016	0.038	0.029	0.049	0.070	0.025	0.007	0.075	0.061	0.078	0.036
Fe^{2+}	0.251	0.239	0.085	0.074	0.072	0.165	0.227	0.187	0.122	0.216	0.130	0.161	0.243	0.287	0.121	0.197
Mn	0.007	0.006	0.005	0.005	0.004	0.006	0.007	0.005	0.004	0.010	0.005	0.006	0.013	0.010	0.005	0.005
Mg	0.814	0.812	0.978	0.952	0.952	0.829	0.832	0.866	0.894	0.781	0.871	0.914	0.841	0.815	0.885	0.950
Ca	0.852	0.848	0.834	0.876	0.868	0.974	0.868	0.889	0.811	0.862	0.951	0.871	0.779	0.757	0.818	0.763
Na	0.024	0.024	0.009	0.015	0.013	0.005	0.009	0.008	0.027	0.026	0.005	0.009	0.024	0.027	0.026	0.017
Mg#	76.7	64.5	86.5	88.9	88.9	82.0	75.8	80.4	83.9	73.1	84.9	84.4	72.5	70.1	81.6	80.3
Al^{VI}/Al^{IV}	0.76	0.54	0.19	0.23	0.10	0.04	0.18	0.32	0.39	0.15	0.19	0.57	0.06	0.18	0.23	0.24

Formulae calculated on the basis of 4 cations and 6 oxygens. CG = cumulus gabbro, IG = isotropic gabbro. Mg# = 100*Mg/(Mg + Fe^{2+}).

ticularly to the low temperature alteration amphiboles confined at the grain periphery (Table 2). In the isotropic gabbros igneous magnesiohornblende was preserved only in the samples vs-617 and vs-331 showing similar composition to the magnesiohornblende from cumulus rocks (Table 2, Fig. 5).

Most measured feldspars show albite composition ($An_{0.2-2.7}$; Table 3). Relic igneous plagioclase in cumulate gabbros shows the most Ca-rich composition ($An_{88.7-92.9}$). In the isotropic gabbros plagioclase is systematically lower in Ca and, although homogeneous, individual grains in a sample may show significant composition variations ($An_{23.6-59.9}$ in the sample vs-578).

Magmatic Fe-Ti-oxides are magnetite-ulvöspinel solid solutions (Table 4). In most samples they now contain a net of very fine exsolved lamellae and patches. EPMA spot measurement yields mixed analyses for the exsolved minerals which may be interpreted as magnetite and pseudobrookite.

The Mt Medvednica gabbroic rocks are severely altered showing two distinct alteration assemblages. The chemical

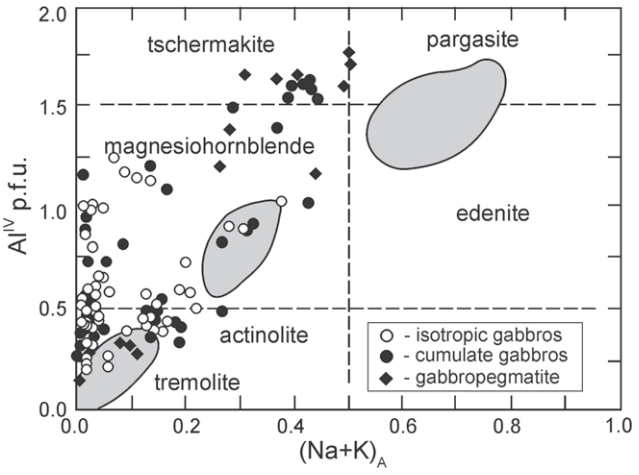

Fig. 5. Al^{IV}–$(Na+K)_A$ plot of amphiboles from the Mt Medvednica gabbroic rocks with the nomenclature fields of Leake et al. (1997). Amphiboles from the Mt Medvednica ultramafic cumulates (Lugović et al. 2007) are shown for comparison (shaded fields).

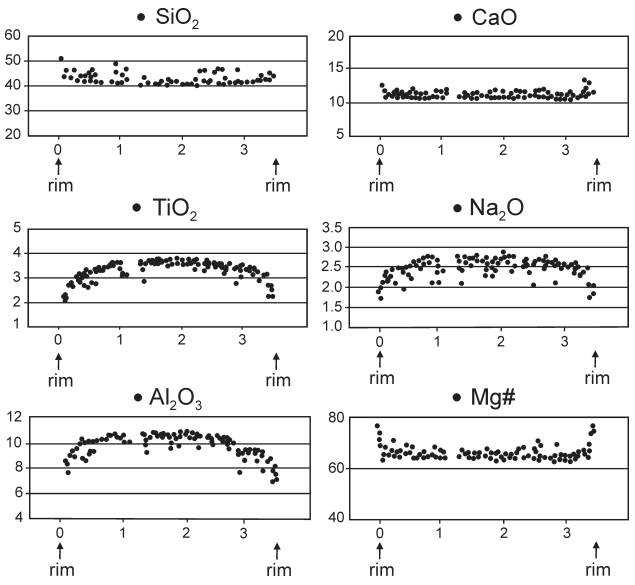

Fig. 6. Compositional zoning patterns of a tschermakite megacryst from the Mt Medvednica gabbropegmatite (sample mc-pg). All spot analyses from the profile resembling alteration composition were omitted for simplicity. Oxides are in wt. % and grain size in millimeters.

Table 2: Selected microprobe analyses and formulae of amphibole from the gabbroic rocks in the Mt Medvednica ophiolite mélange.

Sample	mc-16	mc-16	mc-16	vs-386	vs-386	m-16/2	m-16/2	vh-617	vh-617	vh-617	vs-331	vs-331	vs-331	vs-494	vs-494	mc-pg	mc-pg	mc-pg
Anal. No.	1	3	4	21	5	19	5	16	1	2	6	1	4	16	10	18	14	17	19
Rock type	CG				CG		CG		IG			IG			IG		GPG		
SiO_2	44.31	47.56	52.28	44.83	54.09	51.03	52.18	53.03	47.46	49.17	51.59	48.79	46.56	50.60	51.02	54.40	42.32	44.06	44.06
TiO_2	3.17	1.65	0.37	2.84	0.24	0.46	0.16	0.19	1.74	1.39	0.15	1.22	1.68	0.63	0.18	0.06	3.77	2.99	3.27
Al_2O_3	9.64	6.96	3.54	9.43	3.82	5.46	4.28	3.83	6.74	6.32	4.26	6.17	7.69	5.20	4.34	2.45	11.14	9.84	9.93
Cr_2O_3	0.30	0.00	0.05	0.19	0.17	0.66	0.00	0.05	0.11	0.24	0.09	0.09	0.05	0.05	0.00	0.00	0.07	0.03	0.01
Fe_2O_3	4.99	7.23	1.32	4.93	0.00	0.33	1.40	0.29	1.44	0.46	2.16	1.13	1.58	2.22	2.98	0.00	7.13	7.39	7.91
FeO	7.34	7.29	12.77	7.25	6.63	6.47	9.31	10.04	9.65	9.84	8.34	11.63	11.50	9.11	10.37	10.93	5.88	6.68	5.84
MnO	0.13	0.32	0.27	0.18	0.14	0.02	0.20	0.22	0.16	0.12	0.20	0.19	0.23	0.20	0.20	0.30	0.14	0.17	0.08
MgO	13.89	13.90	14.29	14.24	19.67	19.05	17.92	18.05	16.11	16.72	18.02	15.38	14.67	17.16	17.32	16.80	14.06	13.82	13.99
CaO	11.07	10.93	11.14	11.22	12.01	11.81	10.91	10.83	11.40	11.37	11.24	11.21	11.00	11.31	9.36	11.79	11.09	11.02	10.97
Na_2O	2.23	1.53	0.41	2.26	0.66	1.02	0.50	0.45	1.20	1.02	0.58	0.97	1.18	0.65	0.18	0.18	2.71	2.39	2.11
K_2O	0.11	0.09	0.02	0.14	0.04	0.10	0.06	0.04	0.13	0.12	0.15	0.07	0.10	0.09	0.05	0.03	0.10	0.11	0.11
H_2O	2.05	2.07	2.05	2.06	2.14	2.10	2.09	2.10	2.05	2.07	2.09	2.05	2.03	2.09	2.06	2.09	2.07	2.07	2.08
Total	99.23	99.53	98.52	99.56	99.61	98.50	99.01	99.12	98.19	98.84	98.88	98.91	98.27	99.31	98.06	99.03	100.48	100.57	100.35
Cations	6	6	4	6	5	5	5	5	5	5	5	5	5	5	5	5	6	6	6
Si	6.472	6.905	7.635	6.520	7.585	7.286	7.472	7.573	6.957	7.117	7.407	7.124	6.875	7.270	7.416	7.796	6.133	6.377	6.365
Ti	0.348	0.180	0.041	0.311	0.025	0.049	0.017	0.020	0.192	0.151	0.016	0.134	0.187	0.068	0.020	0.006	0.411	0.325	0.355
Al	1.659	1.191	0.609	1.617	0.631	0.919	0.722	0.645	1.164	1.078	0.721	1.062	1.338	0.881	0.743	0.414	1.903	1.678	1.691
Cr	0.035	0.000	0.006	0.022	0.019	0.075	0.000	0.006	0.013	0.027	0.010	0.010	0.006	0.006	0.000	0.000	0.008	0.003	0.001
Fe^{3+}	0.549	0.790	0.145	0.539	0.000	0.035	0.150	0.031	0.159	0.050	0.234	0.124	0.175	0.240	0.326	0.000	0.778	0.805	0.859
Fe^{2+}	0.896	0.885	1.560	0.882	0.778	0.772	1.115	1.199	1.184	1.191	1.002	1.421	1.420	1.095	1.260	1.310	0.713	0.808	0.705
Mn	0.016	0.039	0.033	0.022	0.017	0.003	0.024	0.027	0.020	0.015	0.024	0.023	0.029	0.024	0.025	0.036	0.017	0.021	0.010
Mg	3.024	3.009	3.111	3.088	4.112	4.055	3.825	3.843	3.521	3.608	3.857	3.348	3.229	3.675	3.753	3.589	3.038	2.982	3.013
Ca	1.732	1.700	1.743	1.748	1.804	1.807	1.674	1.657	1.791	1.763	1.729	1.754	1.740	1.741	1.458	1.810	1.722	1.709	1.698
Na	0.632	0.431	0.116	0.637	0.179	0.282	0.139	0.125	0.341	0.286	0.161	0.275	0.338	0.181	0.051	0.050	0.761	0.671	0.591
K	0.020	0.017	0.004	0.026	0.007	0.018	0.011	0.007	0.024	0.022	0.027	0.013	0.019	0.016	0.009	0.005	0.018	0.020	0.020
Mg#	0.771	77.3	66.6	77.8	84.1	84.0	77.4	76.2	74.8	75.2	79.4	70.2	69.5	77.0	74.9	73.3	81.0	78.7	81.0

Formulae calculated on the basis of 23 oxygens and fixed number of 13 cations excluding Ca, Na and K (6), 15 cations excluding Na and K (5) or 15 cations excluding K (4) to match the best amphibole crystalochemical parameters. Estimated H_2O corresponds 2 (OH) per formula unit. Mg# = Mg/(Mg + Fe^{2+}). CG = cumulate gabbro, IG = isotropic gabbro, GPG = gabbropegmatite.

compositions of secondary amphiboles are displayed in Table 2, other secondary minerals in Table 4. Older alteration is typical of the greenschist facies and includes albite, actinolite plus chlorite (clinochlore, penninite and diabantite) and serpentine after magmatic plagioclase, clinopyroxene and/or tschermakite-magnesiohornblende and cumulus olivine. Subsequent alteration comprises prehnite, pumpellyite, titanite and muscovite (sericite). Pumpellyite is Al-rich (Table 4), typical of pumpellyite after plagioclase (Aldahan 1989; Izhizuka 1991) indicating alteration grade between zeolite and greenschist facies. Titanite shows a high rate of Al and lower of Fe^{3+} substitution (Table 4), consistent with the composition of titanite from prehnite-pumpellyite facies alterations (Coombs et al. 1976; Mével 1981).

Bulk-rock chemistry

Chemical analyses of the Mt Medvednica gabbroic rocks are shown in Table 5. High values for LOI (2.12–4.52 wt. %) combined with petrographic evidence suggest that the igneous composition of the rocks may have been changed through successive alterations including weathering.

In spite of the alterations, all analysed rocks plot in the field of sub-alkali gabbros (Fig. 7A). The diagram TiO_2–Al_2O_3 (Fig. 7B) distinguishes between cumulates and basaltic liquid composition, which is more suitable for altered rocks. Cumulus rocks resemble the composition of olivine gabbros and troctolites, whereas isotropic rocks plot in the field of clinopyroxene-plagioclase gabbros. The rocks have low CaO/Al_2O_3 ratio (0.44–0.82) typical of ophiolitic gabbros (Werner 1984). In the AFM diagram (Fig. 8) cumulates occupy the field of Mg-gabbros while isotropic gabbros are scattered in the field of ophiolitic basalt suggesting that the latter rocks may represent liquid composition. High Mg# (76.8–85.3 vs. 62.3–75.6) and wide range of Al_2O_3 (10.71–16.68 wt. % vs. 15.19–17.10 wt. %) in the cumulate rocks relative to the isotropic varieties (Table 5) are strongly controlled by the modal ratio of cumulus minerals and intercumulus amphibole in the former, and by similar modal mineral abundances in the latter.

Crystallization of amphibole in arc-related cumulates will not deplete the liquid in Zr, but will in the Sc, Ti and V (Meurer & Claeson 2002) and therefore the slight increase in Zr in the Mt Medvednica isotropic gabbros

Table 3: Selected microprobe analyses and formulae of feldspars from the gabbroic rocks in the Mt Medvednica ophiolite mélange.

Sample	mc-16	m-16/2	m-16/2	vs-386	vs-617	vs-331	vs-494	vs-578	vs-578	vs-578	mc-pg	mc-pg
Anal. No.	9	7	20	3	3	26	17	10	8	17	6	8
Rock type	CG	CG		CG	IG	IG	IG	IG			GPG	
SiO_2	68.82	45.88	44.53	64.44	66.53	66.47	69.26	52.81	59.75	61.77	68.82	68.89
Al_2O_3	19.96	34.44	34.89	21.19	20.16	20.55	19.41	28.39	25.62	23.77	19.68	19.84
Fe_2O_3	0.16	0.57	0.61	0.77	0.21	0.20	0.01	1.03	0.38	0.74	0.00	0.16
CaO	0.41	17.86	18.62	0.29	0.84	1.04	0.27	12.62	7.52	4.86	0.05	0.16
Na_2O	11.53	1.25	0.79	10.92	11.40	11.28	11.88	4.64	7.18	8.69	12.00	11.87
K_2O	0.03	0.02	0.04	0.97	0.06	0.10	0.05	0.05	0.07	0.22	0.05	0.02
Total	100.91	100.02	99.48	98.58	99.20	33.17	100.88	99.54	100.52	100.05	100.60	100.94
Si	2.980	2.114	2.069	2.884	2.942	2.928	3.000	2.414	2.651	2.743	2.990	2.984
Al	1.019	1.870	1.911	1.118	1.051	1.067	0.991	1.529	1.340	1.244	1.008	1.013
Fe^{3+}	0.005	0.020	0.021	0.026	0.007	0.007	0.000	0.036	0.013	0.025	0.000	0.005
Ca	0.019	0.882	0.927	0.014	0.040	0.049	0.013	0.618	0.358	0.231	0.002	0.007
Na	0.968	0.112	0.071	0.948	0.977	0.963	0.998	0.411	0.618	0.748	1.011	0.997
K	0.002	0.001	0.002	0.055	0.003	0.006	0.003	0.003	0.004	0.012	0.003	0.001
Total	4.993	4.998	5.002	5.045	5.020	5.020	5.004	5.011	4.983	5.003	5.013	5.007
An	1.9	88.8	92.9	1.4	3.9	4.8	1.2	60.0	36.7	23.6	0.2	0.7

Formulae calculated on the basis of 8 oxygens and total Fe as trivalent. CG = cumulus gabbro, IG = isotropic gabbro, GPG = gabbropegmatite. An = 100*Ca/(Ca + Na + K).

Table 4: Selected microprobe analyses and formulae of chlorite, prehnite, pumpellyite, magnetite-ulvöspinel, muscovite and titanite from the gabbroic rocks in the Mt Medvednica ophiolite mélange.

Mineral	Chlorite				Prehnite				Pumpellyite			Mgt	Ms	Ttn
Sample	m-16/2	vs-386	vs-494	vs-578	m-16/2	vs-331	mc-16	mc-pg	vh-617	vs-386	vs-494	vs-578	vs-386	mc-pg
Anal. No.	12	17	14	11	11	5	17	27	5	27	20	16	11	24
Rock type	CG	CG	IG	IG	CG	IG	CG	GPG	IG	CG	IG	IG	CG	GPG
SiO_2	28.79	33.70	30.36	32.29	43.36	42.33	43.99	44.18	37.31	38.04	37.99	0.10	47.99	31.05
TiO_2	0.04	0.03	0.04	0.02	0.01	0.00	0.01	0.00	0.00	0.03	0.00	21.71	0.03	36.01
Al_2O_3	18.90	14.34	17.79	17.10	23.13	24.30	23.15	23.45	27.42	28.30	26.92	2.86	33.86	2.30
Cr_2O_3	0.05	0.42	0.20	0.03	0.00	0.01	0.03	0.00	0.00	0.00	0.04	0.06	0.00	0.06
Fe_2O_3	–	–	–	–	1.29	0.67	0.51	0.73	2.63	1.45	3.16	22.71	–	0.79
FeO	15.23	9.12	14.64	26.75	–	–	–	–	–	–	–	51.32	0.84	–
MnO	0.13	0.39	0.18	0.28	0.10	0.00	0.01	0.10	0.17	0.56	0.12	0.00	0.13	0.00
MgO	23.33	28.11	22.96	10.79	0.07	0.05	0.00	0.12	2.15	1.14	1.88	0.00	1.70	0.00
CaO	0.13	0.23	0.30	0.57	26.59	26.13	26.61	25.92	22.97	23.23	22.89	0.17	0.17	28.40
Na_2O	–	–	–	–	0.05	0.17	0.04	0.07	0.08	0.31	0.20	–	0.23	–
K_2O	–	–	–	–	0.01	0.01	0.00	0.01	0.00	0.01	0.00	–	9.18	–
H_2O	11.90	12.28	11.94	11.49	4.30	4.27	4.31	4.33	5.54	5.58	5.57	–	4.51	–
Total	98.49	98.62	98.41	99.30	98.91	97.94	98.66	98.91	98.28	98.64	98.77	98.93	98.65	98.60
Si	2.902	3.290	3.049	3.369	3.022	2.973	3.061	3.061	3.026	3.065	3.068	0.004	3.190	1.023
Ti	0.003	0.002	0.003	0.001	0.000	0.000	0.001	0.000	0.000	0.002	0.000	0.612	0.001	0.892
Al	2.246	1.650	2.105	2.103	1.900	2.012	1.898	1.915	2.622	2.687	2.562	0.126	2.652	0.089
Cr	0.004	0.032	0.016	0.002	0.000	0.000	0.002	0.000	0.000	0.000	0.003	0.002	0.000	0.002
Fe^{3+}	–	–	–	–	0.068	0.035	0.027	0.038	0.161	0.088	0.192	0.641	–	0.020
Fe^{2+}	1.284	0.745	1.230	2.334	–	–	–	–	–	–	–	1.609	0.046	–
Mn	0.011	0.032	0.015	0.025	0.006	0.000	0.001	0.006	0.011	0.038	0.008	0.000	0.007	0.000
Mg	3.507	4.092	3.437	1.678	0.007	0.006	0.000	0.012	0.260	0.136	0.226	0.000	0.169	0.000
Ca	0.014	0.024	0.032	0.063	1.986	1.966	1.984	1.924	1.996	2.005	1.980	0.007	0.012	1.003
Na	0.000	0.000	0.000	0.000	0.006	0.023	0.005	0.009	0.012	0.049	0.031	–	0.030	–
K	0.000	0.000	0.000	0.000	0.001	0.001	0.000	0.001	0.000	0.001	0.000	–	0.778	–
Total	9.970	9.867	9.887	9.577	6.997	7.016	6.978	6.967	8.089	8.071	8.069	3.000	6.887	3.029
Mg#	73.2	84.6	73.7	41.8	–	–	–	–	–	–	–	–	–	–

Mgt = magnetite-ulvöspinel, Ms = muscovite, Tnt = titanite. CG = cumulus gabbro, IG = isotropic gabbro, GPG = gabbropegmatite. Formulae calculated on the basis of 14 oxygens and all Fe as divalent for chlorite; 11 oxygens and all Fe as trivalent for prehnite; 12.5 oxygens and all Fe as trivalent for pumpellyite; 4 oxygens and 3 cations for magnetite-ulvöspinel; 11 oxygens and all Fe as divalent for muscovite; 5 oxygens and all Fe as trivalent for titanite. H_2O is calculated and corresponds to 8 (OH), 2 (OH), 3 (OH) and 2 (OH) per formula unit in chlorite, prehnite pumpellyite and muscovite, respectively. Mg = 100*Mg/(Mg + Fe^{2+}).

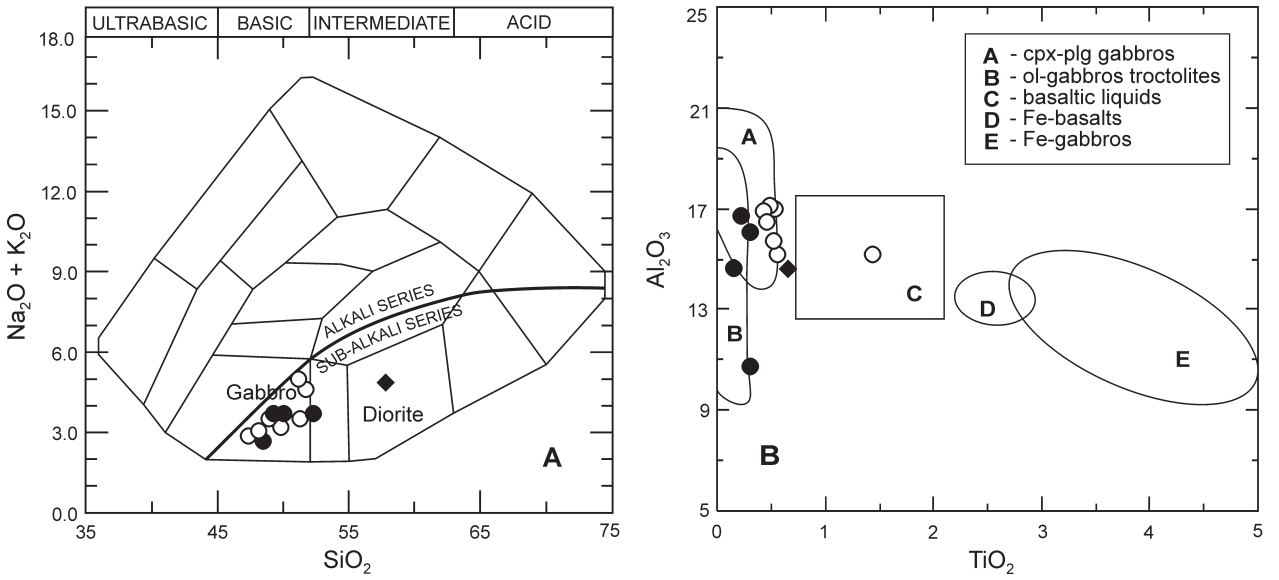

Fig. 7. (**A**) TAS classification diagram with the nomenclature fields of intrusive rocks after Cox et al. (1979) and **(B)** Al_2O_3–TiO_2 discrimination diagram (adopted from Colombi 1989) for the gabbroic rocks from the Mt Medvednica ophiolite mélange. Symbols as in the Fig. 5.

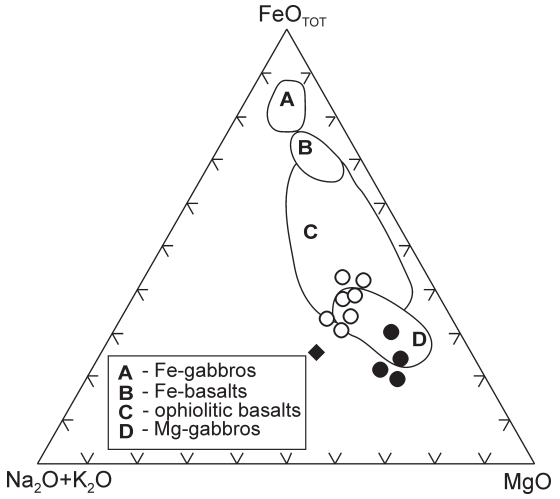

Fig. 8. A–F–M [(Na_2O+K_2O)–FeO_{total}–MgO] diagram (from Bianchi et al. 1998, slightly modified by Colombi 1989) for the gabbroic rocks from the Mt Medvednica ophiolite mélange. Symbols as in the Fig. 5.

(Table 2) may reflect clinopyroxene fractionation. This is corroborated by the Sc/Yb ratio ranging from 9 to 73. Thus, we used Zr as a potential differentiation index to test the behaviour of selected compatible elements (Sc, V, Ni and Cr) and incompatible elements (Ti and La) in the analysed rocks (Fig. 9A–F). In the isotropic gabbros Sc is negatively correlated with Zr (Fig. 9A) whilst V and Ti tend to be positively correlated (Fig. 9B and 9C). Since V and Ti are highly compatible with clinopyroxene in tholeiitic melt their inconsistent behaviour in the analysed rocks suggests that the distribution of V is also strongly controlled by the crystallization of coexisting Fe-Ti-oxide. The amount of Ni decreases in the evolved isotropic gabbros due to cessation of olivine fractionation (Fig. 9D). The low concentration of Cr in the isotropic gabbros (Fig. 9E) reflects the high partition of Cr in spinel and clinopyroxene of underlying cumulus ultramafic rocks (Lugović et al. 2007). La is strongly positively correlated with Zr (Fig. 9F) suggesting that La was not significantly affected by alterations. In short, the HFSE and REE may be used in petrogenetic and geotectonic constraints.

N-MORB normalized multielement concentrations of the gabbroic rocks from the Mt Medvednica are displayed in the spider diagrams (Fig. 10A). The samples show high LILE (Cs, Ba, Rb, K) enrichment and, excluding strong Sr spike, have a nearly flat profile for more compatible elements with higher relative concentrations in isotropic gabbros, which is consistent with their higher degree of fractionation. Compared to the compatible elements, the LILE could be affected during alterations and weathering. We plotted LILE concentrations against Zr and found scattered distributions (not shown) suggesting that the LILE were not enriched to such an extent only by magmatic processes. It particularly holds true for Sr, at least for the isotropic gabbros, since they show early plagioclase fractionation through negative Eu anomaly (Fig. 10B2). Amongst the HFSE, Nb and Ta show significant negative anomalies for cumulate and isotropic gabbros [$(Nb/La)_{MORBN}$ = 0.40–0.72 and 0.28–0.35, respectively] typical for subduction related rocks. Ti may be relatively enriched or depleted (Fig. 10A). The cumulate and early fractionated isotropic gabbros have low abundances of Ti (0.15 wt. % TiO_2 in the sample vs-386 vs. 0.47 wt. % TiO_2 in the sample vs-494) resulting from Ti enrichment in the amphibole oikocrystals of underlying ultramafic cumulates (Lugović et al. 2007) which is typical of suprasubduction cumulate gabbros (Saunders et al. 1980). Positive Ti anomalies in late isotropic mafic rocks (1.44 wt. % TiO_2 in the sample vs-331) are connected to the onset of Fe-Ti-oxides (Elthon 1991).

The REE contents of the gabbroic rocks from the Mt Medvednica normalized to N-MORB concentrations are

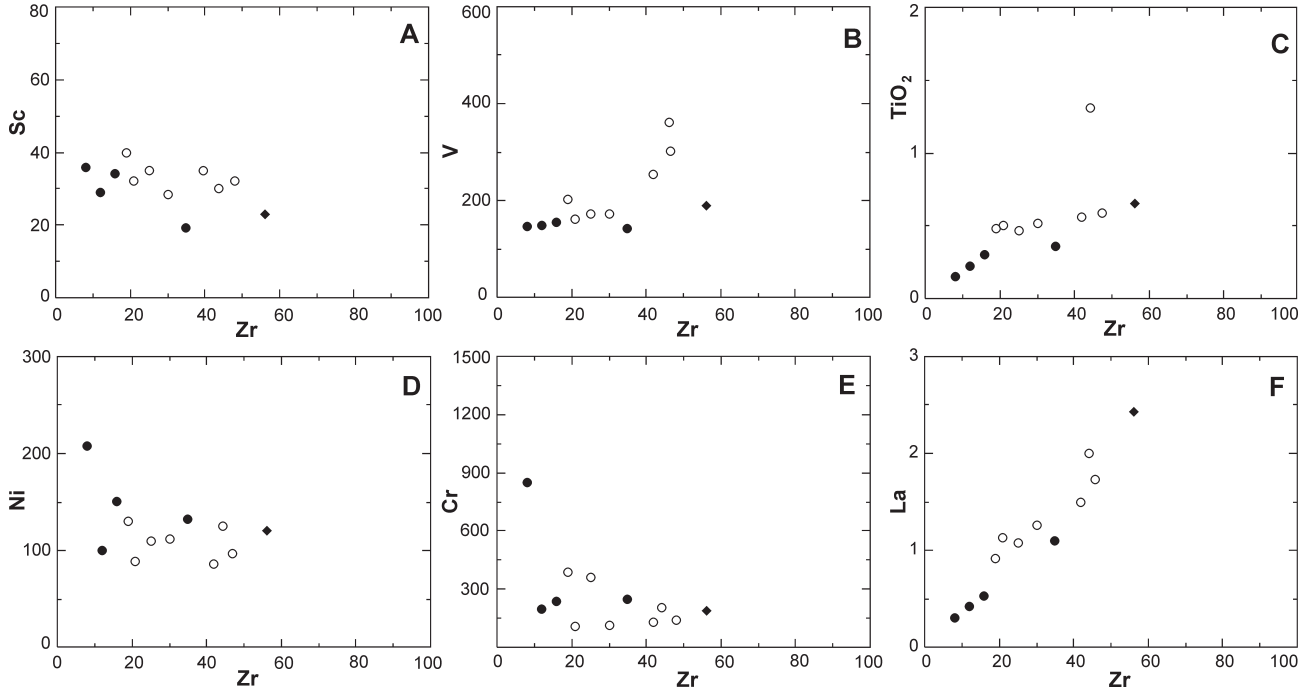

Fig. 9. Variation diagrams for selected elements with Zr as an index of the fractionation index for the Mt Medvednica gabbroic rocks. **A** — Sc–Zr, **B** — V–Zr, **C** — TiO_2–Zr, **D** — Ni–Zr, **E** — Cr–Zr and **F** — La–Zr. Symbols as in the Fig. 5.

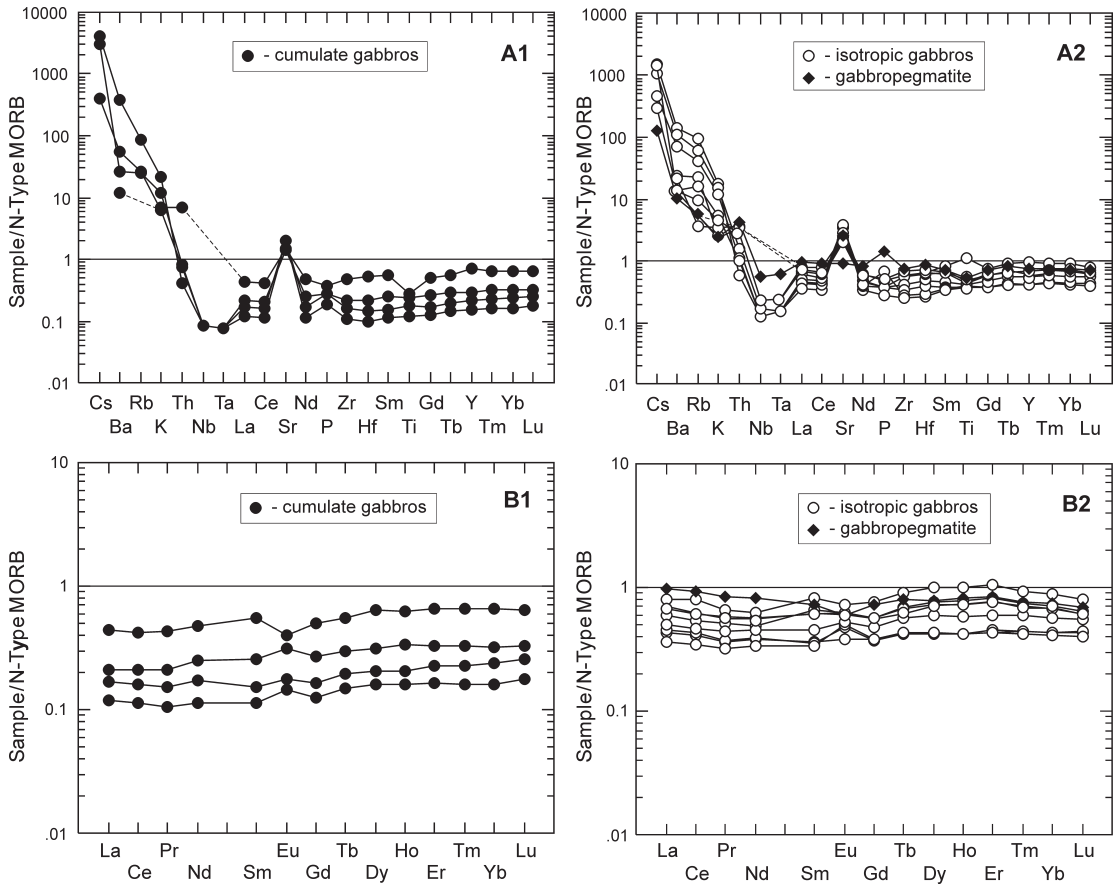

Fig. 10. N-MORB-normalized **(A)** multielement and **(B)** REE patterns for the Mt Medvednica gabbroic rocks. Normalization values are from Sun & McDonough (1989).

Table 5: Chemical analyses of gabbroic rocks from the Mt Medvednica ophiolite mélange.

	Gabbro cumulates				Isotropic gabbros							GPG
Sample	*mc-2/4*	**mc-16**	*vs-367*	*vs-386*	*rn-13*	*vh-617*	*vk-298*	**vs-331**	**vs-335**	*vs-494*	*vs-801*	*mc-pg*
SiO_2	48.52	50.09	52.32	49.29	51.22	48.97	48.50	47.40	49.90	51.71	51.28	57.81
TiO_2	0.30	0.36	0.22	0.15	0.52	0.48	0.57	1.44	0.56	0.47	0.50	14.60
Al_2O_3	16.01	10.71	16.68	14.66	16.98	17.10	15.51	15.19	15.20	16.46	16.92	0.66
$Fe_2O_{3\ total}$	6.72	7.74	5.54	4.88	6.72	6.68	8.95	10.70	10.07	6.45	8.53	4.64
MnO	0.13	0.14	0.09	0.15	0.13	0.13	0.15	0.13	0.13	0.13	0.15	0.10
MgO	11.12	5.17	10.73	13.03	6.82	8.18	9.02	9.09	8.35	8.70	7.85	6.82
CaO	9.42	8.75	7.49	8.20	7.72	9.81	11.05	9.78	9.67	7.20	9.09	8.52
Na_2O	2.28	3.24	2.86	2.15	3.96	2.27	2.82	2.71	3.01	3.79	3.18	4.74
K_2O	0.45	0.05	0.86	1.58	1.11	1.29	0.30	0.19	0.25	0.85	0.40	0.18
P_2O_5	0.03	0.04	0.03	0.02	0.04	0.03	0.05	0.05	0.04	0.04	0.07	0.15
LOI	4.52	4.15	3.92	4.29	4.41	3.89	2.88	3.55	2.45	3.55	2.54	2.12
Total	99.49	100.44	100.76	98.40	99.63	98.84	99.80	100.23	99.63	99.36	100.50	100.30
Mg#	76.8	79.5	82.7	85.3	66.9	70.8	66.8	64.3	62.3	75.6	66.7	75.2
Cs	2.8	11.2	21.5	29.2	7.6	10.8	5.1	3.3	1.1	3.2	2.1	0.9
Rb	15	<2	14	49	34	54	5	13	<2	23	9	3
Ba	350	76	168	2370	682	872	79	152	134	440	89	64
Th	0.09	0.84	0.10	0.05	0.19	0.07	0.31	0.42	0.44	0.13	0.12	0.50
Ta	0.01	<0.10	0.01	0.01	0.02	0.02	0.03	<0.10	<0.10	0.02	0.02	0.08
Nb	0.2	<2.0	0.2	0.2	0.4	0.3	0.5	<2.0	<2.0	0.3	0.3	1.3
Sr	130	135	183	184	322	307	199	215	181	342	252	82
Zr	16	35	12	8	30	19	47	44	42	25	21	56
Hf	0.5	1.1	0.3	0.2	1.0	0.6	1.4	1.3	1.3	0.8	0.6	1.8
Y	8	20	6	4	15	12	18	27	17	12	11	21
Sc	34	18	29	36	26	40	30	36	32	35	32	23
V	155	126	148	146	172	202	298	389	253	172	161	190
Cr	240	246	180	870	115	390	160	250	130	360	110	190
Co	31	25	32	34	28	30	35	39	36	30	32	23
Ni	151	132	100	220	112	130	102	139	86	110	80	120
La	0.53	1.10	0.42	0.30	1.26	0.91	1.73	2.00	1.50	1.08	1.13	2.43
Ce	1.56	3.12	1.20	0.85	3.51	2.59	4.59	5.95	4.02	3.07	3.21	6.95
Pr	0.28	0.57	0.20	0.14	0.58	0.42	0.73	0.87	0.67	0.48	0.49	1.10
Nd	1.84	3.45	1.25	0.83	3.29	2.43	4.04	4.52	3.57	2.80	2.83	5.92
Sm	0.67	1.45	0.40	0.30	1.20	0.88	1.60	2.17	1.72	0.96	0.92	1.89
Eu	0.321	0.41	0.179	0.150	0.538	0.509	0.611	0.74	0.64	0.384	0.485	0.612
Gd	0.98	1.83	0.61	0.46	1.75	1.39	2.02	2.81	2.10	1.40	1.36	2.64
Tb	0.20	0.37	0.13	0.10	0.38	0.29	0.41	0.60	0.46	0.29	0.28	0.54
Dy	1.43	2.94	0.93	0.73	2.73	1.96	3.24	4.53	3.50	1.97	1.91	3.56
Ho	0.34	0.63	0.21	0.16	0.59	0.42	0.73	1.02	0.78	0.42	0.42	0.83
Er	0.98	1.97	0.67	0.49	1.77	1.28	2.29	3.13	2.42	1.33	1.29	2.49
Tm	0.150	0.30	0.104	0.074	0.270	0.193	0.310	0.42	0.34	0.204	0.200	0.349
Yb	0.98	2.00	0.72	0.49	1.72	1.25	2.03	2.72	2.16	1.32	1.31	2.27
Lu	0.150	0.29	0.116	0.081	0.250	0.181	0.270	0.36	0.29	0.202	0.195	0.316

Major elements in wt.%, trace elements in ppm. GPG = gabbropegmatite. LOI = loss on ignition at 1100 °C. Mg# = 100*molar MgO/($MgO+FeO_{total}$). Analyses obtained at Actlabs laboratories indicated by the italic sample lebels.

Table 6: $^{40}Ar/^{39}Ar$ data of gabbropegmatite amphibole from the Mt Medvednica ophiolite mélange.

Step	**Temp. (°C)**	**Time (min.)**	**$^{40}Ar/^{39}Ar$[a]**	**$^{38}Ar/^{39}Ar$[a] $\times 10^{-2}$**	**$^{37}Ar/^{39}Ar$[a]**	**$^{36}Ar/^{39}Ar$[a] $\times 10^{-3}$**	**^{39}Ar[a,b] $\times 10^{-15}$**	**Cumulative ^{39}Ar (%)**	**Radiogenic[c] ^{40}Ar (%)**	**Apparent Age[d] ±2 σ s.d. (Ma)**
1	750	15	29.41	10.07	0.5900	50.06	12.91	25.5	49.7	92.9±1.3
2	950	15	29.69	13.35	3.360	13.00	13.85	52.9	87.8	162.7±1.0
3	1010	15	29.52	54.95	14.63	17.51	12.98	78.6	86.3	160.5±1.2
4	1050	15	27.79	58.76	11.23	14.72	5.643	89.8	87.4	153.0±2.1
5	1150	15	33.43	70.75	16.46	38.25	3.052	95.8	69.9	148.1±4.4
6	1300	15	41.12	121.0	23.23	68.52	2.095	99.9	55.1	144.6±6.4
7	1450	15	1309	157.8	11.55	4409	0.030	100.0	0.5	43.0±2690

[a] Corrected for background (mean values in mol: m/e40 = 1.4×10^{-16}; m/e39 = 7.6×10^{-17}; m/e38 = 3.5×10^{-17}; m/e37 = 5.4×10^{-17}; m/e36 = 5.5×10^{-17}), mass discrimination (measured $^{40}Ar/^{36}Ar$ = 293.5±0.5), abundance sensitivity (5 ppm), and radioactive decay. [b] Normalized to 100% delivery to mass spectrometer. [c] Includes static blank. [d] Corrected for atmospheric argon and nucleogenic interferences $^{40}Ar/^{39}Ar_K$ = 0.0306; $^{36}Ar/^{37}Ar_{Ca}$ = 0.00027; $^{39}Ar/^{37}Ar_{Ca}$ = 0.00077). J-factor = 0.004683 (assumed Fish Canyon Tuff sanidine = 28.02 Ma; Renne et al. 1998).

shown in Fig. 10B. The normalizing REE patterns are parallel at different concentration levels with the higher level in the isotropic gabbros suggesting persistently constant modal composition of the fractioned phases and, consequently, accumulation by different settling rate rather than by change in the settling mineral assemblage. All samples show REE patterns transitional between mid-ocean ridge and island arc plutonic rocks. The cumulus gabbros have a slightly depleted HREE profile whereas the early fractionated isotropic gabbros show an almost flat HREE profile [$(Tb/Lu)_{MORBN}$ from 0.76 to 0.91 vs. 0.94–1.13]. The evolved isotropic gabbros display concave-down HREE profile. The cumulus rocks exhibit flat to slightly LREE enriched profiles [$(La/Nd)_{MORBN} = 0.85$ to 1.05], while the isotropic gabbros show pronounced LREE enrichment [$(La/Nd)_{MORBN} = 1.09–1.29$]. The concave-down shaped MREE profile of the REE patterns reflects amphibole fractionation through the cumulate sequence. The intensity of the Eu-anomaly (Eu/Eu*) decreases from the early cumulates (1.07–1.18) through isotropic gabbros down to 0.86.

$^{40}Ar/^{39}Ar$ dating of gabbropegmatite

The analytical data from laser incremental heating of the amphibole separate are detailed in Table 6 and ^{39}Ar release spectra are shown in Fig. 11. The apparent ages increase over the first heating step to attain maximum apparent ages for the middle half of the age spectrum and then decrease over the last few steps. Plateau age calculated by the criteria of Ludwig (2003) is 161.1 ± 2.1 Ma. We interpreted the plateau age as the age of gabbropegmatite crystallization. This calendar age of gabbropegmatite crystallization corresponds almost exactly to the boundary between the Callovian and Oxfordian (see in Ogg 2004).

Discussion

The mafic cumulate fragments from the Mt Medvednica ophiolite mélange comprise amphibole olivine gabbro and amphibole gabbro. Amphibole gabbro intersected by minor amphibole pegmatitic gabbro dominates amongst isotropic (noncumulate) rocks. On account of cumulate rock mineral composition and rock type the Mt Medvednica mafic intrusive association is an analogue of the Type III arc cumulate suite defined by Beard (1986) from arc intrusive complexes of Bear Mountain, Adak and Lesser Antilles. The observed crystallization sequence is olivine, augite-diopside, Ca-plagioclase and minor magnetite-ulvöspinel as cumulus phase followed by tschermakite-magnesiohornblende and plagioclase as intercumulus fillings (Fig. 2A and 2B). The crystallization sequence is typical of fractionation of tholeiite basalts under low to medium pressure (Serri 1980) in suprasubduction settings and is atypical for mafic rocks from an ocean ridge (Pearce et al. 1984). Maximum crystallization pressure and temperature were inferred as 0.55 GPa and 850 °C, respectively, using semiquantitative thermobarometer calibrated by Ernst & Liu (1998) based on the Al- and Ti contents in tschermakite. This all suggests that the magma crystallized Mt Medvednica amphibole gabbro probably underwent fractional crystallization in a high-level magma chamber.

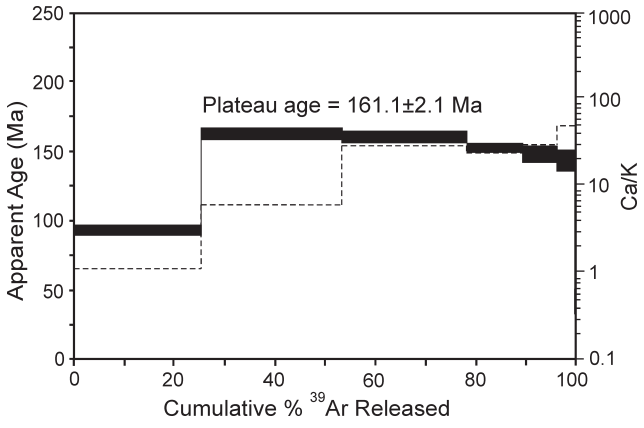

Fig. 11. $^{40}Ar/^{39}Ar$ apparent age diagram of gabbropegmatite amphibole separate from the Mt Medvednica ophiolite mélange.

Abundant tschermakite-magnesiohornblende throughout the gabbroic sequence as well as in the ultramafic cumulates from Mt Medvednica (Lugović et al. 2007) indicates volatile influenced early crystallization. In texture and chemical composition these amphiboles undoubtedly resemble amphiboles defined as magmatic in the ophiolitic gabbros (e.g. Coogan 2003). The ophiolitic mafic-ultramafic rocks associations crystallized from volatile-rich magmas are almost exclusively found in subduction zones, either in island arcs or continental margins (Conrad & Kay 1984; DeBari & Coleman 1989; Claeson & Meurer 2004; Kocak et al. 2005) suggesting the formation of the Mt Medvednica ophiolite plutonic sequences in an analogue of recent/ancient suprasubduction setting. The normal zoning of igneous tschermakite (Fig. 6) indicates crystallization in a closed system (Stern 1979). The relatively low Ti- and Al abundances and apparent chemical homogeneity of cumulus augite suggest slow cooling at elevated pressure.

However, amphibole gabbros may also occur on the mid-ocean ridges. In the MORB setting, formation of Ti-pargasite-tschermakite is confirmed in the late-magmatic evolution of an intrusive sequence as *low abundant* interstitial feelings, blebs and as replacive or vein minerals (Tribuzio et al. 2000; Coogan et al. 2001). In suprasubduction ridge ophiolites like at Oman, magmatic amphibole may be abundant in cumulate gabbros (Coogan 2003) or in gabbroic dikes as large poikilitic patches associated with similar orthopyroxene and clinopyroxene patches (Bosch et al. 2004). The Mt Medvednica amphibole cumulates and isotropic gabbros are thus in this respect more akin to the latter.

The peculiar lithology of the Mt Medvednica gabbroic suite is pegmatitic gabbro composed of secondary albite and well preserved igneous tschermakite. Such pegmatitic occurrences were repeatedly attributed to the interaction of magma with seawater infiltrated down to the magma chamber, which in the case of the Trinity Ophiolite Complex (California) was as deep as close to Mohorovičić discontinuity (Boudier et al. 1989). However, for augite-tschermakite gabbropegmatites

hosted in gabbro from Szarvaskő Ophiolite Complex, Bükk Mountains in NE Hungary, assimilation of sedimentary rocks increasing volatile content in the gabbro magma chamber was attributed to cause local crystallization of gabbropegmatite (Péntek et al. 2006). This gabbropegmatite shows deuteric and low temperature amphibole alterations similar to Mt Medvednica gabbropegmatite but along with host gabbros shows less intensity of albitization. We have found Boudier et al.'s (1989) explanation more acceptable for the Mt Medvednica oceanic crust and, moreover, suggest that the sea water, warmed during downward percolation through the crust, is also responsible for the severe alterations, particularly albitization of the entire rock pile to the mineral assemblage analogue of greenschist facies. The prehnite-pumpellyite facies alteration is clearly successive to the greenschist facies mineral paragenesis and we address its formation to the ophiolite emplacement. In the Szarvaskő gabbropegmatite Péntek et al. (2006) inferred a temperature of 250–400 °C for sea-floor alteration paragenesis, and 270–285 °C at 0.15–0.2 GPa for the prehnite-pumpellyite facies alteration assemblage.

In severely altered ophiolitic rocks clinopyroxene is often the only mineral that preserves an igneous composition. This fact was proved to introduce clinopyroxene as a robust geochemical tracer of the original tectonic setting of the host

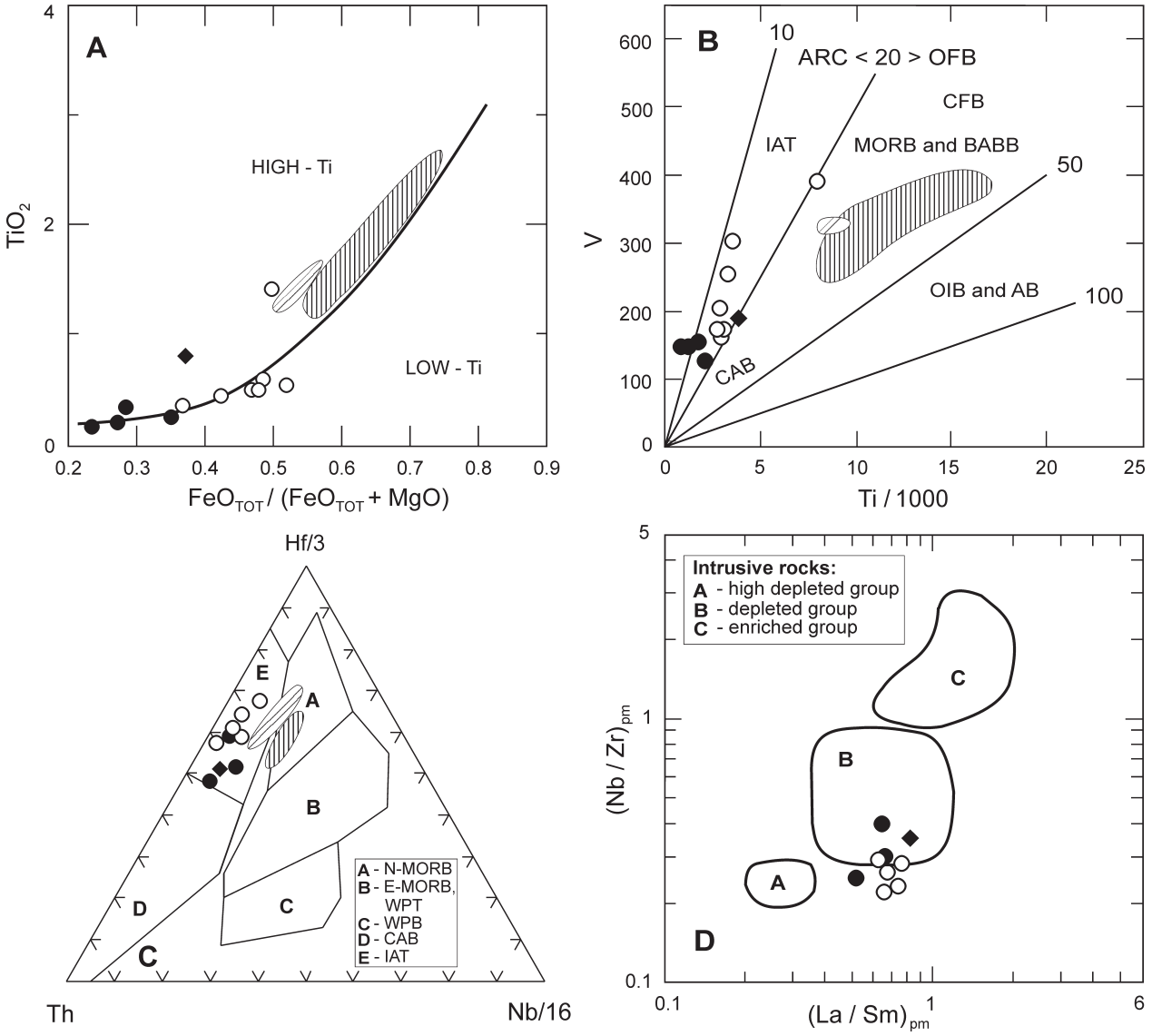

Fig. 12. Discrimination diagrams for the gabbroic rocks from the Mt Medvednica ophiolite mélange. **A** — TiO_2–FeO_{total}/(FeO_{total}+MgO) diagram (Serri 1981). **B** — V–Ti/1000 diagram (Shervais 1982). IAT = island-arc tholeiites, MORB = mid-ocean ridge basalts, BABB = back-arc basin basalts, CAB = calc-alkaline basalts, CFB = continental flood basalts, OIB = ocean-island basalts and AB = alkali basalts. **C** — Th–Hf/3– Nb/16 diagram (Wood 1980). N-MORB = normal mid-ocean ridge basalts, E-MORB = enriched MORB, WPT = within plate tholeiites, WPB = alkaline within plate basalts, CAB = calc-alkaline basalts and IAT = island-arc tholeiites. **D** — $(Nb/Zr)_{pm}$–$(La/Sm)_{pm}$ diagram (Révillon et al. 2000). Normalized values for primitive mantle (pm) are from Hofmann (1988). Symbols and fields as in the Fig. 3. Fields for isotropic gabbros of Szarvaskő Ophiolite Complex (Aigner-Torres & Koller 1999 and Downes et al. 1990) and basalts from the Jaklovce Formation (Ivan 2002) are plotted for correlation constraints.

rock (Beccaluva et al. 1989). Clinopyroxene from the Mt Medvednica amphibole gabbros plotted in discriminatory diagrams shows clear compositional correspondence with clinopyroxenes from modern ocean island arc magmatic rocks (Fig. 4A and 4B). The composition of the relic plagioclase in the Mt Medvednica cumulus gabbros (Table 3) is consistent with clinopyroxene composition. Such high Ca-plagioclase coexisting with amphibole is typically found in the island arc cumulates (e.g. Burns 1985) as a consequence of crystallization from water saturated melts (Arculus & Wills 1980).

Many discriminant diagrams were introduced to distinguish between ophiolitic volcanic rocks from different tectonic settings (Fig. 12). The diagrams are also used for discrimination of plutonic rock but, only if they represent the melt, that is they are not cumulates. The diagrams were devised for fresh rocks of known tectonic position and should be used with caution for altered rocks. Since the Mt Medvednica gabbroic rocks are severely altered we only use elements which were proved to resemble magmatic interelement ratios. The majority of the analysed rocks correspond to high Mg-gabbros (Fig. 8) and show geochemical trend typical of low-Ti gabbro suites (Fig. 12A). Low-Ti gabbros are assumed to be highly representative of suprasubduction ophiolites and particularly of island arc ophiolites (Serri 1981). The island arc affinity of the Mt Medvednica gabbros is confirmed in the classical discrimination diagram Ti-V (Shervais 1982) where the gabbros plot within the field of island arc tholeiites (Fig. 12B). However, beside gabbropegmatite, one gabbro (sample vs-331) is Ti- and V-enriched and therefore more akin to the ocean ridge gabbro. Since this sample contains an unusually high amount of exsolved Fe-Ti-oxides (former magnetite-ulvöspinel) it is interpreted as an integral part of the suprasubduction suite rather than ridge gabbro. The island arc environment of analysed rocks is fully confirmed by their plot in the diagram Th–Hf/3–Nb/16 (Fig. 12C) where the analysed rocks plot in the tholeiitic field of island arc magmatic rocks. Mantle wedge source for these rocks was only slightly depleted (Fig. 12D), which is also suggested by the element relations from the REE patterns (Fig. 10). Transitional harzburgites representing mantle residium after approximately 20% partial melting exposed near Gornje Orešje several kilometers to the east of the Mt Medvednica ophiolite mélange (Lugović et al. 2007) appear to be the best candidate for the mantle wedge of the Mt Medvednica island arc.

Ophiolite mélanges from the SW ZMTDZ exposed in the Mts Medvednica, Kalnik and Ivanščica (Fig. 1) were regarded by Haas et al. (2000) as a single tectonostratigraphic unit, namely the Kalnik Unit (KU). We assumed that the KU contains ophiolitic rock fragments of a discrete Mesozoic oceanic domain, hereafter termed the Repno oceanic domain (ROD), as originally proposed by Babić et al. (2002). The formation of MORB-type oceanic crust in the ROD commenced in the late Ladinian (Halamić et al. 1998; Goričan et al. 2005) and is clearly traced during the Upper Triassic (Halamić & Goričan 1995). The formation of MORB-type gabbros and dolerites continued from Pliensbachian to the Bajocian as documented by K-Ar bulk-rock isotopic ages (Pamić 1997). The youngest MORB-type crust may be recognized in the pillow lavas exposed adjacent to the Lower Callovian cherts (Halamić et al. 1999). If the ophiolitic rock fragments from the Mt Medvednica mélange resemble remnants of the same slow-spreading (~1.5 mm/yr) oceanic domain which was continously producing oceanic crust from the late Ladinian to the Early Callovian, then oceanic crust about 900 km wide must have been formed.

An intraoceanic subduction leads to formation of an accretionary wedge in front of a fore-arc–arc system (Wilson 1989). The commencement of intra-oceanic subduction in the ROD is not clear. Most probably subduction/accretionary wedge started to form soon after Bajocian-Early Callovian when the youngest ridge crust was documented (Pamić 1997; Halamić et al. 1999). The accretionary wedge in the ROD corresponds to the KU sensu Haas et al. (2000) and to the chaotic Repno Complex sensu Babić et al. (2002). The age of the Repno Complex was constrained to Early Callovian to Late Valanginian (Babić et al. 2002) and the lower age matches well the assumed age of the cessation of ridge crust formation. However, Babić et al. (2002) do not link the Repno Complex to an intra-oceanic setting but to the "eastern" continental margin (Tisia?). The existence of a post Bajocian-Lower Callovian fore-arc, that is a proto-arc sensu Woodhead et al. (1998) in the ROD may be envisaged from the ultramafic cumulate rock fragments archived in the Mt Medvednica ophiolite mélange and transitional tectonite peridotites from Gornje Orešje (Lugović et al. 2007). During the time of around 15 Ma, a fore-arc progrades to an island arc with coeval cognate back-arc basin (Stern & Bloomer 1992; Bloomer et al. 1995). Following this model we link the Mt Medvednica gabbropegmatite, which crystallized 161.1 Ma ago, to an early suprasubduction stage, namely to the proto-arc setting. Our amphibole gabbroic rocks clearly testify for the progradation of that proto-arc and formation of ophiolites in an island arc setting. The ROD island arc never prograded to maturity as it may be concluded from the total absence of calc-alkaline rocks in the mélange. We adopt the age span of Babić et al. (2002) for the KU but doubt its proposed setting. Assuming our approach is correct, the age of duration of the subduction factory producing the ROD proto-arc–island arc ophiolites may be extended to the Late Valanginian. Cognate back-arc ophiolites were not recognized among the ophiolitic rock fragments in the ROD yet.

The closure of the ROD arc–back-arc system was completed rapidly during the Barremian–Aptian by the obduction of the ROD island arc onto the Adria continental platform and resulted in formation of the Mt Medvednica orthogreenschists (Lugović et al. 2006) 118 Ma BP (Belak et al. 1995). The initiation of closure of the potential cognate ROD back-arc basin may be inferred from the amphibolites in the metamorphic sole in Mt Kalnik. These amphibolites metamorphosed 118 Ma BP from back-arc ridge tholeiite basaltic and gabbro protoliths (Šegvić et al. 2005; Ignjatić 2007).

In modern island arc–back-arc systems there is a correlation between the rate of subduction and the intensity of back-arc volcanism (Rodkin & Rodkinvo 1996). Island arcs with low subduction rates (3–7 cm/yr) show slight HFSE depletion and low back-arc volcanism, whilst island arcs with high subduction rates (>10 cm/yr) show high HFSE deple-

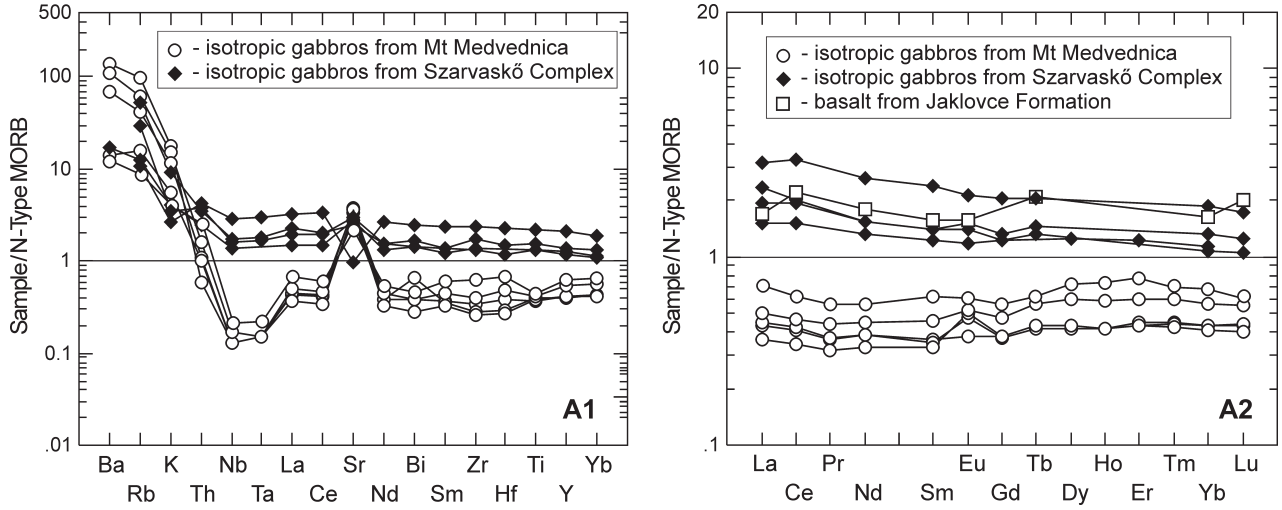

Fig. 13. N-MORB-normalized **(A)** multielement and **(B)** REE patterns for the representative isotropic gabbros from the Mt Medvednica ophiolite mélange compared with gabbroic rocks from Szarvaskő Ophiolite Complex and from the Jaklovce Formation basalts. Data for Szarvaskő are from Aigner-Torres & Koller (1999) and Downes et al. (1990) and for basalts from Jaklovce basalts from Ivan (2002). Normalization values are from Sun & McDonough (1989).

tion (Thirlwall et al. 1994). In the Mt Medvednica isotropic gabbros the intensity of Ta-Nb depletion is significant (Fig. 10A) advocating at least a medium subduction rate. Assuming that the subduction/accretion processes in the ROD were active from after the Early Callovian to the Late Valanginian (Babić et al. 2002), that is around 35 Myr, an impressive amount (~900 km) of MORB-type oceanic crust must have been subducted underneath the Mt Medvednica island arc.

Our data document the establishment of an island arc in the ROD positioned between the Meliata/Maliak ophiolites in the NW and the Dinaric/Vardar ophiolites in the SE (Fig. 1A). With the aim of testing the geochemical affinities of these ophiolites, we have correlated the geochemical characteristics of the amphibole gabbros from the Mt Medvednica ophiolite mélange with selected rocks, thought to be possible equivalents, from the Szarvaskő Ophiolite Complex in the NE part of ZMTDZ and from the Jaklovce Formation of Meliata ophiolites. In the Figs. 3, 4 we compare clinopyroxene from the Mt Medvednica gabbros, Szarvaskő gabbros (Balla & Dobretsov 1984) and Jaklovce basalts since these gabbroic rock were not reported by analyses (Hovorka & Spišak 1988; Ivan 2002). The liable data for the correlation of gabbroic rocks from the Central Dinaric and Vardar Zone ophiolites are not available. However, there is little doubt about the formation of the Central Dinaric ophiolites in a ridge, either in the middle of an ocean (Trubelja et al. 1995) or possibly in a back-arc (Lugović et al. 1991). The Vardar ophiolites seem to be related to a back-arc basin (see compiled in Pamić et al. 2002). The pyroxene from the Mt Medvednica gabbros shows a distinctive chemical composition compared to clinopyroxene from the relevant ophiolites (Fig. 3) showing a composition akin to clinopyroxene hosted in island arc tholeiitic rocks (Fig. 4). The clinopyroxenes from the Szarvaskő gabbros and Jaklovce basalts show composition similar to clinopyroxenes from magmatic rocks formed in the mid-ocean ridge or back-arc ridge. These observations are consistent with relations in the discriminant and spider diagrams where the Mt Medvednica gabbros are characterized by strong suprasubduction geochemical signatures, typical of island arcs, whereas the Szarvaskő gabbros and Jaklovce basalt show insignificant to slight traces of subduction component (Figs. 12A–C and 13). Therefore, a petrogenetic and consequently geotectonic connection between the Mt Medvednica amphibole gabbros and Szarvaskő ophiolites cannot be postulated. Mt Medvednica gabbros appear to be peculiar ophiolitic rocks which represent remnants of an extinct island arc from the Repno oceanic domain and are not comparable to either rocks reported up to now from the Meliata/Maliak ophiolites and Dinaric/Vardar ophiolites. They should be considered as the marker rock type for geotectonic correlations in the western Tethyan realm, particularly concerning the ophiolites of the Vardar Zone which were assumed to have been formed in a back-arc setting (Pamić et al. 2002). However, a fore-arc–island arc segment of the oceanic system as the source of these ophiolites should not be disregarded (Lugović et al. 2006a).

Conclusions

The analysed amphibole gabbroic rocks intersected by amphibole gabbropegmatite are fragments of a dismembered ophiolite within the Mt Medvednica ophiolite mélange formed between the Early Callovian and the Late Valanginian and positioned in the SW tips of the ZMTDZ, this is the NW part of the Sava Zone. The rocks belong to the Repno oceanic domain located between the Maliak and Dinaric domains.

The gabbros showing a crystallization sequence of olivine, augit-diopside, Ca-plagioclase and magnetite-ulvöspinel embedded in tschermakite-magnesiohornblende in the cumulate

rocks are interpreted to have been formed at low to moderate pressure from wet magmas in a high-level magma chamber.

Geochemical data on mineral and rock chemistry and age determination suggest a proto-arc–immature island arc as the crystallization source of the analysed gabbroic rock fragments. Formation of this system is linked to the Early Callovian to Late Valanginian intra-oceanic subduction in the Repno oceanic domain. The island arc most likely did not evolve to maturity.

The Mt Medvednica amphibole gabbroic rocks experienced ocean-floor greenschist facies alteration by percolating of descending solutions. Prehnite-pumpellyite alterations are addressed to the ophiolite emplacement.

The island arc became extinct during obduction onto the Adria platform and, besides the analysed fragments, was recognized in the Baremian-Aptian greenschist facies orthometamorphic rocks from Mt Medvednica.

The peculiar geochemical characteristics of the analysed amphibole gabbroic rocks promote them as an excellent marker for petrogenetic and geotectonic correlations of suprasubduction ophiolites from the western Tethys, particularly of the Vardar Zone.

Acknowledgments: The presented outcome is the result of the scientific projects "Mesozoic magmatic, mantle and pyroclastic rocks of northwestern Croatia"; Project No. 181-1951126-1141 and "Tectonomagmatic correlation of fragmented oceanic lithosphere in the Dinarides"; Project No. 195-1951126-3205, carried out with the support of the Croatian Ministry of Science, Education and Sport. We thank H-P. Meyer for microprobe facilities and I. Fin for polished thin sections. We appreciate the laboratory assistance of M. Valent, N. Čegec and B. Prša. Critical comments by Z. Jovanović, P. Ivan, B. Tomljenović and an anonymous reviewer greatly helped to improve an earlier version of the manuscript.

References

Aigner-Torres M. & Koller F. 1999: Nature of the magma source of the Szarvaskő complex (NE Hungary): petrological and geochemical constraints. *Ofioliti* 24, 1–12.

Aldahan A.A. 1989: The paragenesis of pumpellyite in granitic rocks from the Siljan area, central Sweden. *Neu. Jb. Mineral. Mh.* 367–383.

Aoki K. & Kushiro I. 1968: Some clinopyroxenes from ultramafic inclusions in Dreiser Weiher, Eifel. *Contr. Mineral. Petrology* 21, 743–749.

Arculus R.J. & Wills K.J.A. 1980: The petrology of plutonic blocks and inclusions from the Lesser Antilles island arc. *J. Petrology* 21, 743–799.

Babić Lj., Hochuli P.A. & Zupanič J. 2002: The Jurassic ophiolitic mélange in the NE Dinarides: Dating, internal structure and geotectonic implications. *Eclogae Geol. Helv.* 95, 263–257.

Baker D.R. & Eggler D.H. 1987: Compositions of anhydrous and hydrous melts coexisting with plagioclase, augite, and olivine or low-calcium pyroxene from one atmosphere to 8 kbar: application to the Aleutian volcanic center of Atka. *Amer. Mineralogist* 72, 12–28.

Balla Z. & Dobretsov N.L. 1984: Mineralogy and petrology of peculiar type ophiolites–magmatic rocks from Szarvaskő (Bükk Mountains, North Hungary). *Ofioliti* 9, 107–122.

Beard J.S. 1986: Characteristic mineralogy of arc-related cumulate gabbros: implications for the tectonic setting of gabbroic plutons and for andesite genesis. *Geology* 14, 848–851.

Beccaluva L., Macciotta G., Piccardo G.B. & Zeda O. 1989: Clinopyroxene composition of ophiolite basalts as petrogenetic indicator. *Chem. Geol.* 77, 165–182.

Belak M., Pamić J., Kolar-Jurkovšek T., Pécskay Z. & Karan D. 1995: Alpine regional metamorphic complex of Mt. Medvednica (northwestern Croatia). In: Vlahović I., Velić I. & Šparica M. (Eds.): Proceedings, 1st Croatian Geological Congress, Opatija, 18–21.10.1995. *Inst. Geol.,* Zagreb, 1, 67–70 (in Croatian).

Bianchi G.W., Martinotti G. & Oberhänsli R. 1998: Metasedimentary cover sequences and associated metabasites in the Sabbione Lake zone, Formazza Valley, Italy, NW Alps. *Schweiz. Mineral. Petrogr. Mitt.* 78, 133–146.

Bloomer S.H., Taylor B., MacLeod C.J., Stern R.J., Fryer P., Hawkins J.V. & Johnson L. 1995: Early arc-volcanism and the ophiolite problem: a perspective from drilling in the western Pacific. In: Taylor B. & Natland J. (Eds.): Active margins and marginal basins of the Western Pacific. *Washington D.C., Amer. Geophys. Union*, 1–30.

Bosch D., Jamais M., Boudier F., Nicolas A., Dautria J.M. & Agrinier P. 2004: Deep and high-temperature hydrothermal circulation in the Oman ophiolite — petrological and isotopic evidence. *J. Petrology* 45, 1181–1208.

Boudier F., Le Seur E. & Nicolas A. 1989: Structure of an atypical ophiolite: the Trinity complex, eastern Klamath Mountains, California. *Geol. Soc. Amer. Bull.* 101, 820–833.

Burns L.E. 1985: The Border Ranges ultramafic and mafic complex, south-central Alaska: cumulate fractionates of island-arc volcanics. *Canad. J. Earth Sci.* 22, 1020–1038.

Claeson D.T. & Meurer W.P. 2004: Fractional crystallization of hydrous basaltic "arc-type" magmas and the formation of amphibole-bearing gabbroic cumulates. *Contr. Mineral. Petrology* 147, 288–304.

Colombi A. 1989: Métamorphism et Géochimie des roches mafiques des Alpes Ouest-centrales (géoprofil Vičge-Domodossola-Locerano). *Mémoires de Géologie (Lausanne)* 4, 1–216.

Conrad W.K. & Kay R.W. 1984: Ultramafic and mafic inclusions from Adak Islands: Crystallisation history, and implications for the nature of primary magmas and crustal evolution in the Aleutian arc. *J. Petrology* 25, 88–125.

Coogan L.A. 2003: Contaminating the lower crust in the Oman ophiolite. *Geology* 31, 1065–1068.

Coogan L.A., Wilson R.N., Gillis K.M. & MacLeod C.J. 2001: Near-solidus evolution of oceanic gabbros: Insights from amphibole geochemistry. *Geochim. Cosmochim. Acta* 65, 4339–4357.

Coombs D.S., Nakamura Y. & Vuagnat M. 1976: Pumpellyite-actinolite facies schist of the Taveyanne formation near Loeche, Valais, Switzerland. *J. Petrology* 17, 440–447.

Cox K.G., Bell J.D. & Pankhust R.J. 1979: The interpretation of igneous rocks. *Allen and Unwin*, 1–450.

Crnković B. 1963: Petrography and petrogenesis of the magmatites of the northern part of Mt. Medvednica. *Geol. Vjes.* 16, 63–160 (in Croatian, English summary).

DeBari S.M. & Coleman R.G. 1989: Examination of deep levels of an island arc: Evidence from the Tonsina ultramafic-mafic assemblage, Tonsina, Alaska. *J. Geophys. Res.* 94, 4373–4391.

Downes H., Pantó Gy., Árkai P. & Thirlwall M.F. 1990: Petrology and geochemistry of Mesozoic igneous rock, Bükk Mountains. *Lithos* 24, 201–215.

Elthon D. 1991: Geochemical evidence for formation of the Bay of Islands ophiolite above a subduction zone. *Nature* 354, 140–143.

Ernst W.G. & Liu J. 1998: Experimental phase-equilibrium study of Al- and Ti contents of calcic amphibole in MORB — A semi-

quantitative thermobarometer. *Amer. Mineralogist* 83, 952–969.

Goričan Š., Halamić J., Grgasović T. & Kolar-Jurkovšek T. 2005: Stratigraphic evolution of Triassic arc-backarc system in northwestern Croatia. *Bull. Soc. Géol. France* 176, 3–22.

Grove T.L., Gerlach D.C. & Sando T.W. 1982: Origin of calc-alkaline series lavas at Medicine Lake Volcano by fractionation, assimilation and mixing. *Contr. Mineral. Petrology* 80, 160–182.

Haas J., Mioč P., Pamić J., Tomljenović B., Árkai P., Bérczi-Makk A., Koroknai B., Kovács S. & Felgenhauer E. 2000: Complex structural pattern of the Alpine-Dinaridic Pannonian triple junction. *Int. J. Earth Sci*. 89, 377–389.

Haas J. & Kovács S. 2001: The Dinaridic-Alpine connection — as seen from Hungary. *Acta Geol. Hung.* 44, 345–362.

Halamić J. 1998: Lithostratigraphic characterisation of Jurassic and Cretaceous sediments with ophiolites at Mts Medvednica, Kalnik and Ivanščica. *Ph.D. Thesis, Univ. Zagreb*, 1–188 (in Croatian, English summary).

Halamić J. & Goričan Š. 1995: Triassic radiolarites from Mts. Kalnik and Medvednica (Northwestern Croatia). *Geol. Croatica* 48, 129–146.

Halamić J., Slovenec Da. & Kolar-Jurkovšek T. 1998: Triassic pelagic limestones in pillow lavas in the Orešje quarry near Gornja Bistra, Medvednica Mt. (Northwest Croatia). *Geol. Croatica* 51, 33–45.

Halamić J., Goričan Š., Slovenec Da. & Kolar-Jurkovšek T. 1999: Middle Jurassic radiolarite-clastic succession from the Medvednica Mt. (NW Croatia). *Geol. Croatica* 52, 29–57.

Herak M. 1999: Tectonic interrelation of the Dinarides and the Southern Alps. *Geol. Croatica* 52, 83–98.

Hofmann A.W. 1988: Chemical differentiation of the Earth: the relationship between mantle, continental crust, and oceanic crust. *Earth Planet. Sci. Lett*. 90, 297–314.

Hovorka D. & Spišak J. 1988: Mesozoic Meliata ocean dismembered ophiolites. In: Rakús M. (Ed.): Geodynamic development of the Western Carpathians. *Geol. Surv. Slovak Rep.,* Bratislava, 81–88.

Ignjatić S. 2007: Lower Cretaceous amphibolites from lherzolite metamorphic sole (Kalnik Mt., Croatia). *Dipl. Thesis, Univ. Zagreb*, 1–61 (in Croatian, English summary).

Ivan P. 2002: Relicts of the Meliata ocean crust: geodynamic implications of mineralogical, petrological and geochemical proxies. *Geol. Carpathica* 53, 245–256.

Izhizuka H. 1991: Pumpellyite from zeolite facies metabasites of the Horokanai ophiolite in the Kamuikotan zone, Hokkaido, Japan. *Contr. Mineral. Petrology* 107, 1–7.

Kocak K., Isık F., Arslan M. & Zedef V. 2005: Petrological and source region characteristics of ophiolitic hornblende gabbros from the Aksaray and Kayseri regions, central Anatolian crystalline complex, Turkey. *J. Asian Earth Sci.* 25, 883–891.

Leake B.E. & group of authors 1997: Nomenclature of amphiboles: Report of the Subcommittee on amphiboles of the International Mineralogical Association, Commission on new minerals and mineral names. *Canad. Mineralogist* 35, 219–246.

Ludwig K.R. 2003: Isoplot 3.09. A geochronological toolkit for Microsoft Excel. *Berkley Geochronology Center*, *Spec. Publ. No. 4*, 1–71.

Lugović B., Altherr R., Raczek I., Hofmann A.W. & Majer V. 1991: Geochemistry of peridotites and mafic igneous rocks from the Central Dinaric Ophiolite Belt, Yugoslavia. *Contr. Mineral. Petrology* 106, 201–216.

Lugović B., Šegvić B. & Altherr R. 2006: Petrology and tectonic significance of greenschists from the Mt. Medvednica (Sava unit, NW Croatia). *Ofioliti* 31, 39–50.

Lugović B., Šegvić B., Babajić E. & Trubelja F. 2006a: Evidence of short-living intaroceanic subduction in the Central Dinarides, Konjuh ophiolite complex (Bosnia-Herzegovina). *Proceedings, International Symposium, Mesozoic Ophiolite Belts of the Northern Part of the Balkan Peninsula, Belgrade-Banja Luka, May 31–June 6, 2006. Serbian Academy of Sciences and Arts & Academy of Sciences and Arts of Republic of Srpska*, 72–75.

Lugović B., Slovenec Da., Halamić J. & Altherr R. 2007: Petrology, geochemistry and geotectonic affinity of the Mesozoic ultramafic rocks from the southwesternmost Mid-Transdanubian Zone in Croatia. *Geol. Carpathica* 58, 511–530.

Meurer W.P. & Claeson D.T. 2002: Evolution of crystallizing interstitial liquid in an arc-related cumulate determined by LA ICPMS mapping of a large amphibole oikocryst. *J. Petrology* 43, 607–629.

Mével C. 1981: Occurrence of pumpellyite in hydrothermally altered basalts from Vema Fracture Zone (Mid-Atlantic Ridge). *Contr. Mineral. Petrology* 76, 386–393.

Morimoto N. 1988: Nomenclature of pyroxenes. *Schweiz. Mineral. Petrol. Mitt*. 68, 95–111.

Ogg J.G. 2004: The Jurassic Period. In: Gradstein F.M., Ogg J.G. & Smith A.G. (Eds.): A geologic time scale. *Cambridge University Press*, 307–343.

Palinkaš L.A., Bermanec V., Moro A., Dogančić D. & Strmić-Palinkaš S. 2006: The northernmost Ni-lateritic weathering crust in the Tethyan domain, Gornje Orešje, Medvednica Mt. *Proceedings, International Symposium, Mesozoic Ophiolite Belts of the Northern Part of the Balkan Peninsula, Belgrade-Banja Luka, May 31–June 6, 2006. Serbian Academy of Sciences and Arts & Academy of Sciences and Arts of Republic of Srpska*, 97–101.

Pamić J. 1997: The northwesternmost outcrops of the Dinaridic ophiolites: a case study of the Mt. Kalnik (North Croatia). *Acta Geol. Hung.* 40, 37–56.

Pamić J. 2000: The Periadriatic-Sava-Vardar Suture Zone. In: Vlahović I. & Biondić R. (Eds.): Proceedings, 2nd Croatian Geological Congress, Cavtat-Dubrovnik, 17–20.5.2000. *Inst. Geol.,* Zagreb, 333–337 (in Croatian, English summary).

Pamić J. 2002: The Vardar Zone of the Dinarides and Hellenides versus the Vardar Ocean. *Eclogae Geol. Helv.* 95, 99–113.

Pamić J. 2003: The allochthonous fragments of the Internal Dinaridic units in the western part of the South Pannonian Basin. *Acta Geol. Hung.* 46, 41–62.

Pamić J. & Tomljenović B. 1998: Basic geological data on the Croatian part of the Mid-Transdanubian Zone as examplified by Mt. Medvednica located along the Zagreb-Zemplen Fault Zone. *Acta Geol. Hung.* 41, 389–400.

Pamić J., Tomljenović B. & Balen D. 2002: Geodynamic and petrogenetic evolution of Alpine ophiolites from the central and NW Dinarides: an overview. *Lithos* 65, 113–142.

Pearce J.A., Lippard S.J. & Roberts S. 1984: Characteristics and tectonic significance of supra-subduction ophiolites. In: Kokelaar B.P. & Howels M.F. (Eds.): Marginal basin geology. *Geol. Soc. London, Spec. Publ.* 16, 74–94.

Péntek A., Molnar F. & Watkinson D.H. 2006: Magmatic fluid segregation and overprinting hydrothermal processes in gabbro pegmatites of the Neotethyan ophiolitic Szarvaskő Complex (Bükk Mountains, NE Hungary). *Geol. Carpathica* 57, 433–446.

Pouchou J.L. & Pichoir F. 1984: A new model for quantitative analyses. I. Application to the analysis of homogeneous samples. *La Recherche Aérospatiale* 3, 13–38.

Pouchou J.L. & Pichoir F. 1985: "PAP" ($\tilde{\phi}$-$\tilde{\rho}$-Z) correction procedure for improved quantitative microanalysis. In: Armstrong J.T. (Ed.): Microbeam analysis. *San Francisco Press*, 104–106.

Renne P.R., Swisher C.C., Deino A.L., Karner D.B., Owens T.L. & DePaolo D.J. 1998: Intercalibration of standards, absolute ages and uncertainties in $^{40}Ar/^{39}Ar$ dating. *Chem. Geol.* 145, 117–152.

Révillon S., Arndt N.T., Chauvel C. & Hallot E. 2000: Geochemical study of ultramafic volcanic and plutonic rocks from Gorgana

Island, Columbia: the plumbing system of an oceanic plateau. *J. Petrol*ogy 41, 1127–1153.

Rodkin M.V. & Rodkinvo A.G. 1996: Origin and structure of back-arc basins: new data and model discussion. *Phys. Earth Planet. Inter.* 93, 123–131.

Saunders A.D., Tarney J., Marsh N.G. & Wood D.A. 1980: Ophiolites as ocean crust or marginal basin crust: a geochemical approach. In: Panayiotou A. (Ed.): *Proc. Int. Ophiolite Conf. Nicosia, Cyprus*, 193–204.

Serri G. 1980: Chemistry and petrology of gabbroic complexes from the Northern Apennine ophiolites. In: Panayiotou A. (Ed.): *Proc. Int. Ophiolite Conf. Nicosia, Cyprus*, 296–313.

Serri S. 1981: The petrochemistry of ophiolitic gabbro-complexes: A key for classification of ophiolites to low-Ti and high-Ti types. *Earth Planet. Sci. Lett*. 52, 203–212.

Shervais J.W. 1982: Ti-V plots and petrogenesis of modern and ophiolitic lavas. *Earth Planet. Sci. Lett.* 59, 101–118.

Slovenec Da. 1998: Ophiolitic rocks in the area of the Bistra Creek on the northern slopes of Mt. Medvednica. *MSc Thesis, Univ. Zagreb*, 1–104 (in Croatian, English summary).

Slovenec Da. 2003: Petrology and geochemistry of the ophiolitic rocks from Medvednica Mt. *PhD Thesis, Univ. Zagreb,* 1–180 (in Croatian, English summary).

Slovenec Da. & Pamić J. 2002: The Vardar Zone ophiolites of Mt. Medvednica located along the Zagreb-Zemplín line (NW Croatia). *Geol. Carpathica* 53, 53–59.

Stern C. 1979: Open and closed system igneous fractionation within two Chilean ophiolites and tectonic implication. *Contr. Mineral. Petrology* 68, 243–258.

Stern R.J. & Bloomer S.H. 1992: Subduction zone infancy: examples from the Eocene Izu-Bonin-Marianas and Jurassic California arcs. *Geol. Soc. Amer. Bull.* 104, 1621–1636.

Sun S.S. & McDonough W.F. 1989: Chemical and isotopic systematics of oceanic basalts: implications for mantle composition and processes. In: Saunders A.D. & Norry M.J. (Eds.): Magmatism in ocean basins. *Geol. Soc. London, Spec. Publ.* 42, 313–345.

Šegvić B., Lugović B. & Ignjatić S. 2005: Petrochemical and geotectonic characteristics of amphibolites from the Zagorje-Mid-Transdanubian shear zone (Mt. Kalnik, Croatia). In: Vlahović I. & Biondić R. (Eds.): Abstract Book, 3rd Croatian Geological Congress, Opatija, 29.09.–01.10.2005. *Croat. Geol. Survey,* Zagreb, 143–144.

Thirlwall M.F., Smith T.E., Graham A.M., Theodoroux N., Hollings P., Davidson J.P. & Arculus R.J. 1994: High field strength element anomalies in arc lavas: source or process. *J. Petrology* 35, 819–838.

Tomljenović B. 2002: Structural characteristics of Medvednica and Samoborsko Gorje Mts. *PhD Thesis, Univ. Zagreb,* 1–206 (in Croatian, English summary).

Tomljenović B., Csontos L., Márton E. & Márton P. 2008: Tectonic evolution of the northwestern Internal Dinarides as constrained by structures and rotation of Medvednica Mts., North Croatia. In: Tectonic Aspects of the Alpine-Carpathian-Dinaride System. *Geol. Soc. London, Spec. Publ.* (in print).

Tribuzio R., Tiepolo M. & Thirlwall M.F. 2000: Origin of titanian pargasite in gabbroic rocks from the Northern Apennine ophiolites (Italy): insights into the late-magmatic evolution of a MOR-type intrusive sequence. *Earth Planet. Sci. Lett.* 176, 281–293.

Trubelja F., Marching V., Burgath K.-P. & Vujović Ž. 1995: Origin of the Jurassic Tethyan ophiolites in Bosnia: a geochemical approach to tectonic setting. *Geol. Croatica* 48, 49–66.

Wass S.Y. 1973: The origin and petrogenetic significance of hourglass zoning in titaniferous clinopyroxenes. *Mineral. Mag.* 39, 133–144.

Werner C.D. 1984: Global evolution of the mafic magmatism with special regard to the rare earth elements. *Miner. Slovaca* 16, 29–37.

Wilson M. 1989: Igneous petrogenesis. *Unwin Hyman Ltd*., London, 1–465.

Woodhead J.D., Eggins S.M. & Johnson R.W. 1998: Magma genesis in the New Britain island arc: further insights into melting and mass transfer processes. *J. Petrology* 39, 1641–1668.